GEOPHYSICAL INVESTIGATIONS AT THE NEZEKAW TERRACE MOUND GROUP (SITE 13AM82), EFFIGY MOUNDS NATIONAL MONUMENT, ALLAMAKEE COUNTY, IOWA

By
Steven L. De Vore

Midwest Archeological Center
Technical Report No. 118

NATIONAL PARK SERVICE
Midwest Archeological Center

GEOPHYSICAL INVESTIGATIONS AT THE NEZEKAW TERRACE MOUND GROUP (SITE 13AM82), EFFIGY MOUNDS NATIONAL MONUMENT, ALLAMAKEE COUNTY, IOWA

By
Steven L. De Vore

Midwest Archeological Center
Technical Report No. 118

NATIONAL PARK SERVICE
Midwest Archeological Center

United States Department of the Interior
National Park Service
Midwest Archeological Center
Lincoln, Nebraska
2009

This report has been reviewed against the criteria contained in 43CFR Part 7, Subpart A, Section 7.18 (a) (1) and, upon recommendation of the Midwest Regional Office and the Midwest Archeological Center, has been classified as

Available

Making the report available meets the criteria of 43CFR Part 7, Subpart A, Section 7.18 (a) (1).

ABSTRACT

The National Park Service's Midwest Archeological Center and Effigy Mounds National Monument staffs with the University of Nebraska-Lincoln graduate student and the Volunteer-In-Parks participants conducted geophysical investigations at the Nezekaw Terrace Mound Group (Site 13AM82) located on the Effigy Mounds National Monument in Allamakee County, Iowa. The geophysical investigations were conducted between June 8 and 14, 2008. The archeological investigations were requested by an anthropology graduate student at the University of Nebraska-Lincoln as part of his Masters Thesis archeological project at Effigy Mounds National Monument. The project was located within the Yellow River or North Unit of the park on the east side of the visitors center above the confluence of the Mississippi River and the Yellow River.

During the investigations, 3,721 square meters or 0.92 acres were surveyed with a single fluxgate gradiometer and a dual fluxgate gradiometer system, a conductivity meter, a resistance meter and twin probe array, and a ground penetrating radar cart system with a 400 mHz antenna. The geophysical project was divided into two units, EFMO1 and EFMO2, which were separated by an upland drainageway. The geophysical data collected at the selected project areas provided information of the physical properties of the subsurface materials. Several geophysical anomalies were identified during the investigation of the two project areas. The resistance, ground penetrating radar, magnetic, and conductivity anomalies represented the outlines of buried mound remnants at EFMO1, while the integrity of the two mounds at EFMO2 was also documented as a result of the magnetic, resistance, and conductivity surveys within the survey area. It is recommended that additional geophysical investigations be undertaken at the Nezekaw Terrace Mound Group to identify buried archeological resources associated with the geophysical anomalies identified at the National Park Service unit.

ACKNOWLEDGEMENTS

This project was completed with the support and assistance from the Effigy Mounds National Monument staff. Sincere appreciation is extended to EFMO Superintendent Phyllis Ewing, EFMO Chief Ranger Kenneth Block, and EMFO Administrative Officer Friday Wiles who assisted in the planning and implementation of the University of Nebraska-Lincoln archeological and geophysical project. All of the EFMO park staff went out of their way to make the MWAC crew and volunteers feel welcome and provided assistance in getting the work done efficiently, safely, and as comfortably as possible during the archeological investigations. I would like to thank Jim Lindsay for the opportunity to work with him on his Masters Thesis project. I would also like to thank the Volunteers-In-Park participants Fred Gee and Gary Dalecky for assisting in the collection of geophysical data and setting out the survey grids and traverse ropes. I would also like to thank Park Rangers Abbey Harkrader, John Eicher, and Daísha Lucas for their assistance in the collection of the resistance and ground penetrating radar data on the EFMO1 geophysical project area.

At the Midwest Archeological Center, I would like to thank Dr. Mark Lynott (MWAC Manager), Dr. Ralph Hartley (MWAC Archeological Assistance and Partnership Program Manager), and Anne Vawser (MWAC Archeological Information Management Program Manager) for their direction, leadership, and support during the project. I am also grateful for the support provided by Administrative Officer Jill Lewis, and the rest of the MWAC staff for all of their help without which this project would not have been completed as smoothly or efficiently as it was. Linda Clarke, Darin Schlake, and Sara Vestecka provided logistical, computer, transportation, and personnel support during the project while Allan Weber and Anna Loach provided editing and report preparation in the publishing of this document. I am grateful for the review comments of the draft manuscript.

TABLE OF CONTENTS

LIST OF TABLES

LIST OF FIGURES

1. INTRODUCTION

The geophysical survey at Effigy Mounds National Monument (EFMO) was conducted as part of the National Park Service's (NPS) Midwest Archeological Center (MWAC) technical support of a University of Nebraska-Lincoln (UN-L) graduate anthropology Masters Thesis research project (De Vore 2008). The geophysical investigations were conducted during the week of June 8 to 14, 2008, in an area to the east of the modern visitors center in the location of the historically documented Nezekaw Terrace Mound Group (Site 13AM82: Nezekaw also spelled Nazekaw) in Allamakee County, Iowa (Figure 1). The geophysical survey included a magnetic survey with dual and single fluxgate gradiometers, a resistance survey with a resistance meter and twin probe array, a conductivity survey with an electromagnetic induction meter (EMI), and a ground penetrating radar survey (gpr) with a gpr cart system and 400 mHz antenna. These techniques offered inexpensive, rapid, and relatively non-destructive and non-invasive methods of identifying buried archeological resources and site patterns, which were detectable and also provided a means for sampling relatively large areas in an efficient manner (Roosevelt 2007:444-445; and Von Der Osten-Woldenburg 2005:621-626). The geophysical survey was conducted in an attempt to identify any remnants of the plowed down mound group on the right side of an upland drainage emptying into the Mississippi River. The geophysical survey was conducted by MWAC archeologist Steven L. DeVore with assistance from UN-L graduate student Jim Lindsay, Volunteer-In-Park (VIP) program participants Fred Gee and Gary Dalecky, and EMFO park staff including Abbey Harkrader, Daísha Lucas, and John Eicher.

Effigy Mounds National Monument was established by a Presidential Proclamation by Harry S Truman on October 25, 1949 under the Antiquities Act of 1906 (Truman 1949). The park encompasses 2,526 acres with more than 200 known prehistoric mounds (HRA Gray & Pape 2003:2-3). The mounds were constructed between 700 and 2,500 years ago. The earthen mounds in the northeastern part of Iowa were described as having "*great scientific interest because of the variety of their forms, which include animal effigy, bird effigy, conical, and linear types, illustrative of a significant phase of the mound-building culture of the prehistoric American Indians*…(Truman 1949). The monument consists of the Jennings-Liebhardt or South, the Yellow River or North, Heritage Addition, and Sny Magill Units. The geophysical project area is located within the Yellow River or North Unit of the park.

2. ENVIRONMENTAL SETTING

Site 13AM82 is located within the Wisconsin Driftless section of the Central Lowland province of the Interior Plains division of the North American continent (Fenneman 1938:518-536). The region is part of the maturely dissected plateau and lowlands invaded by glacial outwash. The region has limited landscape modification from the glacial ice sheets. The site also lies within the western part of the Northern Mississippi Valley Loess Hills land resource region of the Central Feed Grains and Livestock Region major land resource area (USDA 2006:326-328). The region consists of gently sloping to rolling summits with steeper valley walls that occur along small to very large flood plains. Stream valley are narrow, deep, and V-shaped with steep cliffs and irregular slopes. The joint patterns in the underlying bedrock control the local drainage patterns with sharp and abrupt turns. The region is characterized by high bluffs, deep valleys, rock outcrops, caves and crevices, and sinkholes (USDA 2006:326; Vobora 1998:3). The Mississippi River flows through much of the region forming the boundaries between Iowa and Illinois and between Minnesota and Wisconsin (USDA 2006:327).

The area also lies within the Illinoian biotic province (Dice 1943:21-23). The native vegetation is dominated by alternating deciduous forests and prairie (Brown 1985:30-44; Sutton and Sutton 1985:58-70). Hardwood forest occur on the uplands with oak, hickory, and sugar maple forming the dominant species. Prairies contain big bluestem and little bluestem. Dominant species on the lowlands consist of mixed hardwood forests with elm, cottonwood, ash, silver maple, river birch, and willow. Sedge and grass meadows occur in the wetter lowlands (USDA 2006:327). Wildlife in the region includes white-tailed deer, fox, coyote, cottontail rabbit, squirrels, beaver, otter, raccoon, skunk, opossum, muskrat, Canada goose, bald eagle, hawks and falcons, turkey, ruffed grouse, owls, ducks, and a variety of songbirds, reptiles, insects, and aquatic fauna (Brown 1985:39-44; Shelford 1963:89-119,17-55,328-355; Sutton and Sutton 1985: 65-70; USDA 2006:327-328).

Alfisols, Entisols, and Mollisols dominate the soil groups in the region (USDA 2006:327). Parent materials include loess, residuum, alluvium, and glaciofluvial deposits with mixed mineralogy. The loamy soils are dominated by moderately deep to very deep soils which are well drained or moderately well drained. The soils range from level to very steep depending on their topographic setting. The soil temperature is a mesic regime. The soils also have an udic soil moisture regime (USDA 2006:327). The two geophysical project areas within the Effigy Mounds National Monument lie within the Lacrescent-Fayette-Village soil association of *gently sloping to strongly sloping, well drained upland soils formed in silty material* (Vobora 1998:8-9). The EFMO1 geophysical project is located in the mowed lawn behind the park's visitors center. The area slopes to the southeast and to the east ending at the edge of the deciduous forest above the intermittent flooded area adjacent to Bluegill Pond and Yellow River near its confluence with the Mississippi River. The upper portion of the geophysical project area lies within the Zwingle silt loam soil (mapping unit 249C) on one to nine percent slopes (Vobora 1998:108-109). This gently sloping soil occurs on the treads of stream terraces and forms in lacustrine deposits with a native vegetation of deciduous trees. The soil is poorly drained with a very slow permeability and moderate available water capacity. The moderate organic matter content in the surface layer is approximately 2.5 percent. The Medary silt loam soil with 14 to 45 percent slopes (mapping unit 951G) lies on the side and toe slopes of the stream terrace below the elevation of the Zwingle soil in the EFMO1 project area (Vobora 1998:74-76). This steeply sloping soil occurs on the risers of stream terraces and forms in lacustrine deposits with a native vegetation of deciduous trees. The soil is well drained with a slow permeability and high available water capacity. The moderate organic matter content in the surface layer is approximately two percent. The channeled Caneck silt loam soil with zero to two percent slopes (mapping unit 1490) lies at the bottom of the slope within the EFMO1 project area next to Bluegill Pond (Vobora 1998:35-36). The soil forms on the flood plains in calcareous alluvium. This nearly level soil is frequently flooded. The soil is poorly drained with a high available water capacity. The moderately low organic matter content in the surface layer is approximately 1.2 percent. Above the Medary silt loam soil on the northern side of the upland drainage, the EFMO2 geophysical project area lies within the transition zone between the Lacrescent silt loam soil with 25 to 70 percent slopes (mapping unit 840G) lies on upland head, nose, and side slopes and the Medary silt loam soil next to the upland drainage (Vobora 1998:67-70). The project area lies on the terrace bench above the upland drainageway that separated the two geophysical project areas. The Lacrescent steeply sloping soil is well drained and formed in pedisediments with a native vegetation of deciduous trees. The soil is well drained with a moderate to moderately rapid permeability and moderate available water capacity. The high organic matter content in the surface layer is approximately four percent.

The climate is temperate continental with warm, humid summers and cold winters (Dice 1943:22; USDA 2006:281; Trewartha and Horn 1980:299-302; Vobora 1998:3-6). The cold winters are moderately long and relatively severe. Annual precipitation averages 75 cm. Most of the precipitation occurs in the form of rain between April and September. Snowfalls can be heavy with the snow staying on the ground throughout the winter season. The average annual temperature ranges between 2 and 13 degrees C. Temperatures at Waukon range from a January average of -8° C to a July average of 26° C. Extreme temperatures range from a minimum of -35° C to a maximum of 37 C (Vobora 1998:3-6). The region has a freeze free period of approximately 140 days (Vobora 1998:6).

3. CULTURAL RESOURCE INVESTIGATIONS

The cultural resource investigations at the Effigy Mound National Monument have produced numerous archeological reports. The prehistory and history of the area have been consolidated into an archeological overview and assessment of the park (Benn and Stadler 2004) a historic resource study (HRA Gray & Pape 2003), and an administrative history (O'Bright 1989) of the Effigy Mounds National Monument, which formed the basic elements for the archeological resources management within the boundary of the park. A general overview of the park may be found in Dennis Lenzendorf's 2000 guide to the national monument. The first extensive mound investigations in the vicinity of the present park boundaries in northeastern Iowa occurred in the 1880s by Alfred J. Hill and Theodore H. Lewis (Benn and Stadler 2004:4; HRA Gray & Pape 2003:31-34; Lenzendorf 2000:52-56; O'Bright 1989:41-42). Lewis conducted the fieldwork and sent detailed notes back to Hill who compiled the notes into detailed measured drawings. The Lewis-Hill survey maps formed the basis of subsequent mound studies since many of the extent mounds from the 1880s were destroyed or obliterated by agricultural and other activities before the establishment of the national monument. Modern mound studies within the region began in the 1920s under the direction of Dr. Charles R. Keyes, Iowa's first State Archaeologist, and Ellison Orr, Keyes' assistant and supervisor of the Iowa Archeological Survey (Benn and Stadler 2004:5-6; HRA Gray & Pape 2003:42; Lenzendorf 2000:61-76; O'Bright 1989:42-46). Orr resurveyed many of Lewis' original mound investigations, including the Nezekaw Terrace Mound Group (13AM82), and excavated several uninvestigated mounds during his tenure at the Iowa Archeological Survey (Figure 2).

The Nezekaw Terrace is a prominent terrace on the left bank of the Yellow River at its confluence with the Mississippi River (Benn and Stadler 2004:15-17). T. H. Lewis named the terrace in 1892 after the Nazekaw townsite and grist mill at the eastern end of the bluff above the mouth of the Yellow River, which was platted but never developed (Benn and Stadler 2004:31). During his survey of the Nezekaw Terrace in 1892, Lewis identified 63 mounds. The mounds included two bear effigies and three conical mounds, which were reported on his field map. In addition to this mound group, he also reported 39 conical mounds, six compounds, 12 embankments and one ruined tailless animal (Orr 1939:105-107). In 1926, Orr remapped the cultivated terrace, which resulted in the identification of only four conical mounds noted by Lewis (Orr 1939:105-107). NPS archeologist Paul Beaubien located two more linear mounds and two conical mounds in 1950 that were apparently not noticed by Orr in 1926 (Beaubien 1952). Farmstead activities, including agricultural cultivation, had destroyed the majority of mounds identified by Lewis by the time Orr reinvestigated the terrace in 1926. Benn and Stadler (2004:15-17,20) provided a summary of the archeological investigations at the Nezekaw Terrace Mound Group in their archeological overview and assessment of the park.. In 1999, MWAC archeologists Robert Nickel and Scott Stadler (Stadler and Nickel 1999) conducted archeological and geophysical investigations in proposed construction areas near the visitors center for a handicap walkway from the visitors center to a small mound group on the south side of State Highway 76. The geophysical investigations consisted of magnetic surveys of grid units near the visitor's center encompassing a small mound group. The geophysical data indicated the presence of a small mound feature to the west of the group of four mounds. The authors identified the feature as a possible remnant of a small linear mound, which had been disturbed by an old road.

4. GEOPHYSICAL SURVEY METHODOLOGY

The geophysical survey project at the Nezekaw Terrace Mound Group (13AM82) within Effigy Mounds National Monument was conducted in the lawn east of the visitors center, identified as area EFMO1 (Figure 3) and in a timbered area across the upland drainage to the north of EFMO1, which was identified as EFMO2 (Figure 4)). In EFMO1, eight 20-meter by 20-meter grid units, which were used to control the placement of the instruments during data acquisition, were established (De Vore 2008). The project area was placed in the area that Lewis and Orr had identified as the location of a group of mounds including two bears and three conical mounds. These mounds had been leveled by agricultural activities after Lewis first noted them in the 1890s. On the southern facing side slope of the terrace on a level bench, two parallel ruts extend along the bench from the southwest to the northeast. These ruts appeared to be wagon or road ruts that ended at the location of a early 20th century cabin. The outline of the cabin was noted in the 1930 aerial photograph (Jim Lindsay 2008, personal communications). In EFMO2, two 20 m by 20 m grid units were placed over an area encompassing a small conical mound and a larger effigy mound, possibility a bird effigy (De Vore 2008). The small conical mound had a trench through the center of the mound oriented in an east to west direction. The possible bird effigy had been trenched into from the south with a large circular excavation near the center of the mound. The backdirt removed from the mound appeared to have been deposited along the body of the effigy beneath the wing areas. The mounds were bounded on the north and south sides by two roads which were used as farm roads or logging roads in this portion of the park. A large trash dump of historic metal objects was noted on the eastern wing of the effigy and between the eastern wing and the northern road.

The grids were established along an east-west baseline and a north-south baseline using an Ushikata S-25 TRACON surveying compass (Ushikata 2005) and 100-meter tape. The initial mapping station was established at the northwest corner of the geophysical survey area at EFMO1. The east-west baseline along the north side of the project area was set 1.5 meters away from the edge of the mowed lawn next to the timbered area above the right side of the upland drainageway. The line was extended 60 meters to the base of the terrace. Wooden hub stakes were placed at 20-meter intervals along the line. These served as the corner points of the EMFO1 grid units along the north side of the project area. Using this as the initial baseline, the surveying compass was rotated 90 degrees to the south and the east-west baseline along the western edge of the EFMO1 geophysical project area was established and wooden hub stakes were driven in at 20-meter intervals along the baseline to mark the corners of the grid units. The line measured 60 meters. The north-south line was oriented to 23 degrees west of magnetic north in the EFMO1 geophysical project area. The established baseline hubs were used as survey stations for the placement of the remaining grid corner hubs. Six complete and two partial 20-m by 20-m grid units were established for the geophysical survey of the EFMO1 geophysical project area. The total area investigated by the geophysical survey in EMFO1 was 2,921 m^2 or 0.72 acres. The EFMO2 geophysical project area was located approximately 30 north of the northeast corner of EFMO1. The initial mapping station was established at the southeast corner of the geophysical project area on the east side of the small conical mound. Using the surveying compass and 100-m tape, the northeastern grid unit point was located 20 meters north of the southeastern grid unit corner and mapping station. The north-south baseline was oriented on magnetic north. The line extended 20 meters north of the mapping station. A 90-degree angle was turned, and the east-west baseline along the south side of the EFMO2 geophysical project area was extended 40 meters west of the southeastern corner of the project area. Wooden hub stakes were placed at 20 meter intervals. The established baseline hubs were used as survey stations for the placement of the remaining grid corner hubs. Two complete 20-m by 20-m grid units were established for the geophysical survey of the EFMO2 geophysical project area. The total area investigated by the geophysical survey in EMFO2 was 800 m^2 or 0.20 acres. The total geophysical survey area for both project locations was 3,721 m^2 or 0.92 acres.

The geophysical survey grid corner stakes at the two project areas within the Nezekaw Terrace Mound Group (13AM82), were mapped with a Trimble GeoXH global positioning system (gps) handheld receiver and external antenna (Trimble 2007a). The gps readings at stationary points (i.e., grid unit corners and individual surface features) were collected with 30 readings from five or more satellites while line segment data were collected at one second intervals along the path of the line. The field gps data were collected in the universal transverse mercator (UTM) projection for the Zone 15 North coordinates of the North American Datum of 1983 (NAD83) horizontal datum. The data were transferred to a laptop computer via the Trimble TerraSync software (Trimble 2007b,2007c). The data was then differentially corrected using the Trimble Pathfinder Office software (Trimble 2007d) using the continuously operating reference station (CORS) Blue River (BLRW) site located 55 kilometers away at Blue River, Wisconsin (Table 1). Twenty files were processed with 160 (26.5%) of 603 selected positions were code corrected by post-processing and 169 (93.9%) of 180 selected positions were carrier corrected by post-processing with 1 (0.8%) of the code positions chosen over carrier, as it was of higher quality. The estimated range for the 160 corrected positions yielded 0% within an accuracy range of 0-15 cm, 37.5% within and accuracy range of 15-30 cm, 0% within an accuracy range of 30-50 cm, 33.8% within an accuracy range of 0.5-1.0 m, 1.9% within an accuracy range of 1.0-2.0 m, 23.8% within an accuracy range of 2.0-5.0 m, and 3.1% at an accuracy range grater than 5.0 m. The high DOP values resulted from a variety of sources including multi-pathing of the satellite signal through the overhead tree canopy, poor satellite geometry, and the number of satellites present during the collection phase. After the raw survey data in the standard storage format (SSF) was post processed, the corrected data were exported to excel data files and imported into Surfer 8 for final display (Figure 5).

Twenty-meter ropes were placed along the east-west base lines connecting the grid unit corners. These ropes formed the north and south boundaries of each grid unit during the data collection phase of the survey. Additional ropes were placed at one-meter intervals across the grid unit in a north-south orientation (Figure 6). These ropes serve as guides during the data acquisition. The ropes were marked with different color tape at half-meter and meter increments designed to help guide the survey effort. Once the geophysical survey of each grid unit was completed the survey ropes were flipped to the next adjacent grid unit. A sketch map was completed for the two geophysical project areas (Figures 7 and 8). The data were acquired across the grid units beginning in the lower left hand (southwest) corner of each grid unit (Geoscan Research 1987:43-54,2003:5/2-5/11).

EFFIGY MOUNDS

5. GEOPHYSICAL PROSPECTION TECHNIQUES

Geophysical prospection techniques available for archeological investigations consist of a number of techniques that record the various physical properties of earth, typically in the upper couple of meters, however, deeper prospection can be utilized if necessary. Geophysical techniques are divided between passive techniques and active techniques. Passive techniques are primarily ones that measure inherently or naturally occurring local or planetary fields created by earth related processes under study (Heimmer and DeVore 1995:7,2000:55; Kvamme 2001:356,2005:424). The primary passive method utilized in archeology is magnetic surveying. Other passive methods with limited archeological applications include self-potential methods, gravity survey techniques, and differential thermal analysis. Active techniques transmit an electrical, electromagnetic, or acoustic signal into the ground (Heimmer and DeVore 1995:9,2000:58-59; Kvamme 2001:355-356). The interaction of these signals and buried materials produces altered return signals that are measured by the appropriate geophysical instruments. Changes in the transmitted signal of amplitude, frequency, wavelength, and time delay properties may be observable. Active methods applicable to archeological investigations include electrical resistance/resistivity, electromagnetic conductivity (including ground conductivity and metal detectors), magnetic susceptibility, and ground penetrating radar. Acoustic active techniques, including seismic, sonar, and acoustic sounding, have very limited or specific archeological applications. Additional information on the basic geophysical techniques used during the present survey may be found in publications by Drs. Arnold Aspinall, Chris Gaffney, and Armin Schmidt (2008), Dr. Bruce Bevan (1991,1998), Dr. Anthony Clark (2000), Dr. Lawrence B. Conyers (2004), Drs. Lawrence B. Conyers and Dean Goodman (1997), Dr. Andrew David (1995,2001), Drs. Andrew David, Neil Linford, and Paul Linford (2008), Drs. Chris Gaffney and John Gater (2003), Drs. Chris Gaffney, John Gater, and Sue Ovenden (1991,2002), Don H. Heimmer and Steven L. De Vore (1995,2000), Dr. Kenneth Kvamme (2001,2003,2005), Drs. I. Scollar, A. Tabbagh, A. Hesse, and I. Herzog (1990), and Dr. John Weymouth (1986).

Magnetic Survey

A magnetic survey is a passive geophysical survey (see Aspinall et al. 2008; Bevan 1991,1998:29-43; Breiner 1973;1992:313-381; Burger 1992:389-452; Clark 2000:92-98,174-175; Davenport 2001: 50-71; David 1995:17-20; David et al. 2008:20-24; Dobrin and Savit 1988:633-749; Gaffney and Gater 2003:36-42,61-72; Gaffney et al. 1991:6,2002:7-9; Hanson et al. 2005:151-175; Heimmer and DeVore 1995:13,2000:55-56; Kvamme 2001:357-358,2003:441,2005:434-436,2006a:205-233,2006b:235-250; Lowrie 1997:229-306; Milsom 2003:51-70; Mussett and Khan 2000:139-180; Nishimura 2001:546-547; Robinson and Çoruh 1988:333-444; Scollar et al. 1990:375-519; Telford et al. 1990:62-135; Weymouth 1986:343; and Witten 2006:73-116 for more details on magnetic surveying). Two different fluxgate gradiometers were used during the geophysical investigations at Effigy Mounds National Monument. A single fluxgate gradiometer was used to collect magnetic data at the EFMO1 and EFMO2 geophysical project areas. A dual fluxgate gradiometer system was used at the EFMO1 geophysical project area.

A magnetic survey is a passive geophysical prospection technique used to measure the earth's total magnetic field at a point location. Its application to archeology results from the local effects of magnetic materials on the earth's magnetic field. These anomalous conditions result from magnetic materials and minerals buried in the soil matrix. Iron artifacts have very strong effects on the local earth's magnetic field. Other cultural features, which affect the local earth's magnetic field, include fire hearths and soil disturbances (e.g., pits, mounds, wells, pithouses, and dugouts), as well as geological strata. Magnetic field strength is measured in nanoteslas (nT; Sheriff 1973:148). In North America, the earth's magnetic field strength ranges from 40,000 to 60,000 nT with a inclination of approximately 60° to 70° (Milsom 2003:43; Weymouth 1986:341). The project area has a magnetic field strength of approximately 57,400 nT (Peddie 1992; Sharma 1997:72-73) with an inclination of approximately 71° 48' (Peddie and Zunde 1988; Sharma 1997:72-73). Magnetic anomalies of archeological interest are often in the ±5 nT range, especially on prehistoric sites. Target depth in magnetic surveys depends on the magnetic susceptibility of the soil and the buried features and objects. For most archeological surveys, target depth is generally confined to the upper one to two meters below the ground surface with three meters representing the maximum limit (Clark 2000:78-80; Kvamme 2001:358). Magnetic surveying applications to archeological investigations have included the detection of architectural features, soil disturbances, and magnetic objects/artifacts (Bevan 1991; Clark 2000;92-98; Gaffney et al 1991:6; Heimmer and DeVore 1995,2000; Weymouth 1986:343).

Two modes of operation for magnetic surveys exist: the total field survey and the gradient survey. The instrument used to measure the magnetic field strength is the magnetometer (Bevan 1998:20). The total field survey uses a single magnetic sensor. Three different types of magnetic sensors have been used in the magnetometer: 1) proton free precession sensors, 2) alkali vapor (cesium or rubidium) sensors, and 3) fluxgate sensors (for a detailed description of the types of magnetometers constructed from these sensors see Clark 2000:66-71; Milsom 2003:45-47; Scollar et al. 1990:450-469; Weymouth 1986:343-344).

The total field magnetometer is designed to measure the absolute intensity of the local magnetic field. This type of magnetometer utilizes a single sensor. Due to diurnal variation of the earth's magnetic field, the data collected with a single sensor magnetometer must be corrected to reflect these diurnal changes. One method is to return to a known point and take a reading that can be used to correct the diurnal variation. A second method is to use two magnetometers with one operated at a fixed base station collecting the diurnal variation in the magnetic field. The second magnetometer is used to collect the field data in the area of archeological interest. Common magnetometers of this types used in archaeological investigations include the proton precession magnetometer, the Overhauser effect magnetometer (a variation of the proton-precession magnetometer), and the cesium magnetometer.

The magnetic gradient survey is conducted with a gradiometer or a magnetometer with two magnetic sensors at a fixed vertical distance apart. The instrument measures the magnetic field at two separate heights. The top sensor reading is subtracted from the bottom sensor reading. The resulting difference is recorded. This provides the vertical gradient or change in the magnetic field. Diurnal variations are automatically canceled. This setup also minimizes long range trends. The gradiometer provides greater feature resolution and potentially provides better classification of the magnetic anomalies. Two commonly used gradiometers in archeological investigations are the cesium gradiometer and the fluxgate gradiometer. They are capable of yielding 5 to 10 measurements per second at a resolution of 0.1 nT (Kvamme 2001:358). Cesium gradiometers record the absolute total field values like the single sensor total field magnetometers. It also records the gradient change between the bottom and top sensors. The fluxgate sensors are highly directional, measuring only the component of the field parallel to the sensor's axis (Clark 2000:69). They also require calibration (Milsom 2003:46-47). Both cesium and fluxgate gradiometers are capable of high density sampling over substantial areas at a relatively rapid rate of acquisition (Clark 2000:69-71; Milsom 2003:46-47).

The single fluxgate gradiometer, the Geoscan Research FM256 fluxgate gradiometer (Figure 9), is a vector magnetometer, which measures the strength of the magnetic field in a particular direction (Geoscan Research 2006). The FM256 fluxgate gradiometer is an upgraded FM36 fluxgate gradiometer (Geoscan Research 1987) with increased memory capacity and greater down load speed. The sensors must be accurately balanced and aligned along the direction of the field component to be measured. A reference point was selected at each project area for balancing and aligning the gradiometers and for zeroing the conductivity meter. The gradiometer was balanced and the sensors aligned on magnetic north. Grid point N20/E20 was selected for balancing the gradiometers at EFMO1 while the northeast corner of the geophysical grid (grid point N20/E40) was used at EFMO2   The two magnetic sensors in the single fluxgate gradiometer are spaced 0.5 meters apart. The instrument is carried so the two sensors are vertical to one another with the bottom sensor approximately 30 cm above the ground. Each sensor reads the magnetic field strength at its height above the ground. The gradient or change of the magnetic field strength between the two sensors is recorded in the instrument's memory. This gradient is not in absolute field values but rather voltage changes, which are calibrated in terms of the magnetic field. The fluxgate gradiometer provides a continuous record of the magnetic field strength.

The dual fluxgate gradiometer system, the Bartington Grad 601-2 single axis magnetic gradiometer (Figure 10), is also a vector magnetometer, which measures the strength of the magnetic field in a particular direction (Bartington Instruments 2007). The dual fluxgate gradiometer sensor configuration of the instrument uses two fluxgate gradiometer sensor tubes separated by a distance of one meter. The dual gradiometer records two lines of data during each traverse reducing the distance walked and the survey time by half compared to the time and distance covered with a single gradiometer system. The sensors must be accurately balanced and aligned along the direction of the field component to be measured. The reference point for balancing and aligning the dual gradiometer at EFMO1 is same magnetic reference point as used for the single fluxgate gradiometer and aligned on Magnetic North. The fluxgate gradiometer sensor tubes in the dual gradiometer are spaced 1.0 meters apart with the two tubes also spaced at one meter apart. The instrument is carried so the two sensors in each tube are vertical to one another with the bottom sensors approximately 30 cm above the ground. Each sensor reads the magnetic field strength at its height above the ground. The gradient or change of the magnetic field strength between the two vertical sensors is recorded in the instrument's memory for both sensor tubes. These gradients are not in absolute field values but rather voltage changes, which are calibrated in terms of the magnetic field. The dual fluxgate gradiometer also provides a continuous record of the magnetic field strength across each line for each traverse across the grid unit.

The magnetic survey for the single fluxgate gradiometer was designed to collect 8 samples per meter along 1.0-meter traverses or 8 data values per square meter at EFMO1 (Table 2), as well as for the single fluxgate gradiometer survey at EFMO2 (Table 3). The magnetic survey for the dual fluxgate gradiometer was also designed to collect 8 samples per meter along 1.0-meter traverses or 8 data values per square meter at EFMO1 (Table 4). The data were collected in a zig zag fashion with the surveyor alternating the direction of travel along each traverse across the grid. A total of 3,200 data values were collected for each complete 20 by 20 meter grid unit surveyed during the project. The magnetic data were recorded in the memory of the gradiometers and downloaded to a laptop computer at the completion of the survey in each geophysical project area. The magnetic data from the single fluxgate gradiometer were imported into Geoscan Research's GEOPLOT software (Geoscan Research 2003) for processing. Both shade relief and trace line plots were generated in the field before the instrument's memory was cleared. The magnetic data from the dual fluxgate gradiometer were downloaded into the Bartington GRAD 601 software (Bartington 2007). The data were then imported into ARCHAEOSURVEYOR for processing (DW Consulting 2008). Shade and trace plots were generated in the field before the instrument's memory cleared.

Conductivity Survey

The electromagnetic induction (EM or EMI) survey in the conductivity or quadrature phase is an active geophysical technique, which induces an electromagnetic field into the ground (see Bevan 1983,1998:29-43; Clark 2000:171; Clay 2001:32-33,2002; Dalan 1995; Davenport 2001:72-88; David 1995:20; David et al. 2008:34-37; Dobrin and Savit 1988:773-837; Fitterman and Labson 2005:301-355; Gaffney and Gater 2003:42-44; Gaffney et al. 1991:5,2002:10; Heimmer and De Vore 1995:35-41,2000:60-63; Klien and Lajoie 1992:383-535; Kvamme 2001:362-363,2003:441-442; Lowrie 1997:222-228; Mussett and Khan 2000:210-219; Nishimura 2001:551-552; Robinson and Çoruh 1988:490-500; Scollar et al. 1990:520-590; Sharma 1997:265-308; Telford et al. 1990:343-521; Weymouth 1986:317-318,326-327, and Witten 2006:147-213 for more details of electromagnetic induction conductivity surveys). This survey technique measures the apparent soil conductivity, which is in millisiemens per meter (mS/m: Sheriff 1973:197). Conductivity is also the reciprocal of resistivity. The geophysical survey at EFMO1 and EFMO2 is conducted with a Geonics EM38 ground conductivity meter operating in the quadrature phase or conductivity component operating mode (Geonics 1992). The instrument is lightweight and 1.45 meters in length (Figure 11). The self-contained dipole transmitter (primary field source) and self-contained dipole receiver (sensor) coils are located at opposite ends of the meter. The intercoil spacing is 1 meter.

An electromagnetic field is induced into the ground through the transmitting coil. The induced primary field causes an electric current flow in the earth similar to a resistivity survey. In fact, a conductivity survey is the inverse of a resistivity survey. High conductivity equates to low resistivity and vice versa. The materials in the earth create secondary eddy current loops, which are picked up by the instrument's receiving coil. The interaction of the generated eddy loops or electromagnetic field with the earthen materials is directly proportional to terrain conductivity within the influence area of the instrument. The receiving coil detects the response alteration (secondary electromagnetic field) in the primary electromagnetic field. This secondary field is out of phase (quadrature or conductivity phase) with the primary field. The in-phase component of the secondary signal is used to measure the magnetic susceptibility of the subsurface soil matrix. The apparent conductivity data were recorded in units of millisiemens per meter (mS/m). The electrical conductivity unit or siemens is a represents the reciprocal of an ohm-meter (Sheriff 1973:197). The relationship between conductivity and resistivity is represented by the following formula (Bevan 1983; McNeill 1980a): mS/m = 1000/ohm/m.

Changes result from electrical and magnetic properties of the soil matrix. Changes are caused by materials buried in the soil, differences in soil formation processes, or disturbances from natural or cultural modifications to the soil. EM instruments are also sensitive to surface and buried metals. Due to their high conductivity, metals show up as extreme values in the acquired data set. On occasion, these values may be expressed as negative values since the extremely high conductivity signal of the metals cause the secondary coil to become saturated.

In archeology, the instrument has been used to identify areas of compaction and excavation as well as buried metallic objects. It has the potential to identify cultural features that are affected by the water saturation in the soil (Clark 2000; Heimmer and De Vore 1995:35-41). Its application to archeology results from the ability of the instrument to detect lateral changes on a rapid data acquisition, high resolution basis, where observable contrasts exist. Lateral changes in anthropogenic features result from compaction, structural material changes, buried metallic objects, excavation, habitation sites, and other features affecting water saturation (Heimmer and De Vore 1995:37). The conductivity survey can sometimes detect the disturbed soil matrix within the grave shaft. It can also locate large metal objects. Metallic trash on the surface and other small objects buried in the upper portion of the soil can degrade the search of the graves (Bevan 1991:1310).

The EM38 ground conductivity meter was connected to the DL720 Polycorder for digital data acquisition (Geonics 1998). The conductivity survey was designed to collect in the continuous or automatic mode with readings collected every 0.25 second resulting in 4 samples per meter. The data were collected in a parallel fashion or unidirectional mode with the surveyor conducting the data acquisition in the same the direction of travel for each traverse across the grid. The data and header files stored in the polycorder were downloaded into the laptop computer at the end of the survey. The survey of the grid unit began in the lower left hand or southwest corner of the grid. The EM38 was used in the quadrature or conductivity phase, the vertical dipole mode, and one orientation parallel to the direction of travel along the traverses. It provided an exploration depth of approximately 1.5 meters with its effective depth around 0.6 meters in the vertical dipole mode. The instrument was nulled and calibrated before the start of the daily survey at the same point used to balance and align the fluxgate gradiometer.

The conductivity data were collected at a sampling density of 4 samples per meter along every 1.0 meter traverse or 4 samples per square meter in the two geophysical project areas (Tables 5 and 6). A total of 1,600 data measurements were collected for each complete 20 m by 20 m grid unit during the survey. The data were downloaded to a laptop computer at the end of each day's survey effort.

Resistance Survey

The resistance survey is an active geophysical technique, which injects a current into the ground (see Bevan 1991,1998:7-18; Burger 1992:241-318; Carr 1982; Clark 2000:27-63,171-174; Davenport 2001:29-30; David 1995:27-28; David et al. 2008:24-28; Dobrin and Savit 1988:750-773; Gaffney and Gater 2003:26-36,56-61; Gaffney et al. 1991:2;2002:7; Hallof 1992: 39-176; Heimmer and DeVore 1995:29-35,2000:59-60; Kvamme 2001:358-362,2003:441-442,2005:434-436; Lowrie 1997:206-219; Milsom 2003:83-116; Mussett and Khan 2000:181-201; Nishimura 2001:544-546; Robinson and Çoruh 1988:445-478; Scollar et al. 1990:307-374; Sharma 1997:207-264; Somers 2006:109-129; Telford et al. 1990:522-577; Van Nostrand and Cook 1966; Weymouth 1986:318-341; Witten 2006:299-317; and Zonge et al. 2005:265-300 for more details on resistivity surveys). The voltage is measured and by Ohm's Law, one may compute the resistance at any given point (**R=V/I** where **R** is resistance, **V** is voltage, and **I** is current). Due to the problem of contact resistance between two electrodes in the ground, a typical resistance survey makes use of four electrodes or probes. The current passes through two electrodes and the voltage is measured between the other two probes. The configuration of the electrodes also varies (see Milsom 2003:99 and Weymouth 1986:324 for common configurations).

Resistance or resistivity changes result from electrical properties of the soil matrix. Changes are caused by materials buried in the soil, differences in soil formation processes, or disturbances from natural or cultural modifications to the soil. In archeology, the instrument is used to identify areas of compaction and excavation, as well as, buried objects such as brick or stone foundations. It has the potential to identify cultural features that are affected by the water saturation in the soil, which is directly related to soil porosity, permeability, and chemical mature of entrapped moisture (Clark 2000; Heimmer and De Vore 1995:30). Its application to archeology results from the ability of the instrument to detect lateral changes on a rapid data acquisition, high resolution basis, where observable contrasts exist. Lateral changes in anthropogenic features result from compaction, structural material changes, buried objects, excavation, habitation sites, and other features affecting water saturation (Heimmer and De Vore 1995:37). The resistivity survey may sometimes detect the disturbed soil matrix within the grave shaft.

The Geoscan Research RM15 resistance meter uses the PA5 multiple probe array (Geoscan Research 1996). Arranged as a twin probe array, a current and voltage probes are located on a mobile frame, which is moved around the site (Figure 12). Two additional probes are located away from the survey area, which also consist of a current probe and voltage probe. The mobile probes were set 0.5 meters apart on the multiprobe array frame. The remote probes are set a distance 30 times the mobile probe separation. The probes on the frame are located at a fixed distance apart. A general rule of thumb for the depth investigation of resistance survey is the depth is equal to the distance of probe separation. This value is not a unique number but an average for the volume of soil 0.5 meters depth and a surface radius of 0.5 meters under the center point of the instrument frame. The probes are connected to the resistance meter, which is also on the frame. Wings may be added to the frame to expand the separation distance of the probes; however, this requires the resurvey of the grid for each change in the probe separation distance. The measurement is taken when the mobile probes make contact with the ground and complete the electrical circuit. The readings are stored in the resistance meter's memory until downloaded to a lap-top computer.

The resistance survey was designed to collect 2 samples per meter along 1.0-meter traverses or 2 data values per square meter at the two geophysical project areas (Tables 7 and 8). The data were collected in a zigzag fashion with the surveyor maintaining the alternating the direction of travel for each traverse across the grid. A total of 800 data values were collected for a complete 20 meter by 20 meter grid unit with a traverse interval of 1.0 meters. The resistance data were recorded in the memory of the resistance meter and downloaded to a laptop computer at the completion of each day's survey effort. The resistance data were imported into Geoscan Research's GEOPLOT software (Geoscan Research 2003) for processing. Both shade relief and trace line plots were generated before the instrument's memory was cleared.

Ground Penetrating Radar Survey

The ground-penetrating radar (gpr) survey is an active geophysical technique that uses pulses of radar energy (i.e., short electromagnetic waves) that are transmitted into the ground through the surface transmitting antenna (see Annan 2005:357-438; Bevan 1991,1998:43-57; Clark 2000:118-120,183-186; Conyers 2004,2006:131-159,2007:329-344; Conyers and Goodman 1997; Davenport 2001:89-103; David 1995:23-27; David et al.

2008:28-34; Gaffney and Gater 2003:47-51,74-76; Gaffney et al. 1991:5-6,2002:9-10; Goodman et al. 2007:375-394; Heimmer and DeVore 1995:42-47,2000:63-64; Kvamme 2001:363-365,2003:442-443;2005:436-438; Lowrie 1997:221-222; Milson 2003:167-178; Mussett and Khan 2000:227-231; Nishimura 2001:547-551; Scollar et al. 1990:575-584; Weymouth 1986:370-383; and Witten 2006:214-258 for more details on ground-penetrating radar surveys). This radar wave is reflected off buried objects, features, or interfaces between soil layers. These reflections result from contrasts in electrical and magnetic properties of the buried materials or reflectors. The contrasts are a function of the dielectric constant of the materials (Sheriff 1973:51). The depth of the object or soil interface is estimated by the time it takes the radar energy to travel from the transmitting antenna and for its reflected wave to return to the receiving antenna. The depth of penetration of the wave is determined by the frequency of the radar wave. The lower the frequency, the deeper the radar energy can penetrate the subsurface; however, the resulting resolution, or the ability to distinguish objects, features, and soil changes, decreases. These low frequency antennas generate long wavelength radar energy that can penetrate several tens of meters under certain conditions, but can only resolve larger targets or reflectors. The higher the radar wave frequency, the higher the resulting resolution but the penetration depth decreases. High frequency antennas generate much shorter wavelength energy, which may only penetrate a meter into the ground. The generated reflections from these high frequency antennas are capable of resolving objects or features with maximum dimensions of a few centimeters. A resulting tradeoff exists between subsurface resolution and depth penetration: the deeper the penetration then the resulting resolution is less or the higher the resolution then the resulting depth penetration is much shallower.

As radar antenna system (transmitting and receiving antennas) is moved along the survey line, a large number of subsurface reflections are collected along the line. The various subsurface materials affect the velocity of the radar waves as they travel through the ground (Conyers and Goodman 1997:31-40). The rate at which these waves move through the ground is affected by the changes in the physical and chemical properties of the buried materials through which they travel. The greater the contrast in electrical and magnetic properties between two materials at the interface results in a stronger reflected signal. As each radar pulse travels through the ground, changes in material composition or water saturation, the velocity of the pulse changes and a portion of the energy is reflected back to the surface where it is detected by the receiving antenna and recorded by ground-penetrating radar unit. The remaining energy continues to pass into the subsurface materials where it can be reflected by deeper reflectors until the energy finally dissipates with depth. The radar system measures the time it takes the radar pulse to travel to a buried reflector and return to the unit. If the velocity of the pulse is known, then the distance to the reflector or the depth of the reflector beneath the surface can be estimated (Conyers and Lucius 1996).

The success of the survey is dependent on soil and sediment mineralogy, clay content, ground moisture, depth of the archeological resource, and surface topography and vegetation. The ground-penetrating radar signal can be lost or attenuated (i.e., quickly dissipated) in soils that have high moisture content, high electrical conductivity, highly magnetic materials, or high clay contents. Dry soils and sediments, especially those with low clay content, represent the best conditions for energy propagation. A ground-penetrating radar survey, with its capability for estimating the depth and shape of buried objects, may be an extremely valuable tool in the search of grave shafts and trenches. At times, radar cannot profile deep enough or the strata may be so complex as to render the trenches, graves, and other types of excavations indistinguishable from the surrounding soil profile.

The TerraSIRch SIR System-3000 survey cart system (GSSI 2003) operated an antenna at a nominal frequency of 400 megahertz (mHz). The antenna was mounted in a cart that recorded the location of the radar unit along the grid line (Figure 13). The gpr profiles were collected along 0.5 meter traverses beginning in the southwest corner of the grid unit (Table 9). The data were collected in a zigzag or bidirectional fashion with the surveyor alternating the direction of travel for each traverse across the grid. A total of 121 radar profiles were collected across the EFMO1 project area for a distance of 4,228 meters. Ground penetrating radar surveys generally represent a trade-off between depth of detection and detail. Lower frequency antennas permit detection of features at greater depths but they cannot resolve objects or strata that are as small as those detectable by higher frequency antennas. Actual maximum depth of detection also depends upon the electrical properties of the soil. If one has an open excavation, one can place a steel rod in the excavation wall at a known depth and use the observed radar reflection to calibrate the radar charts. When it is not possible to place a target at a known depth, one can use values from comparable soils. Reasonable estimates of the velocity of the radar signal in the site's soil can be achieved by this method (Conyers and Lucius 1996). Using one of the hyperbolas on a radargram profile from the EFMO1 project area (Goodman 2005:76), the velocity was calculated to be approximately 5.5 cm per nanosecond (ns). For a time slice between 5 and 15 ns with the center at 10 ns (two way travel time), the approximate depth to the center of the gpr slice would be 27.5 cm. With a time window of 100 ns, the gpr profile extended to a depth of 2.62 meters.

The TerraSIRch SIR System-3000 survey cart contained a data-logger with a display that allowed the results to be viewed almost immediately after they were recorded (GSSI 2003). The SIR 3000 was set to collect gpr data with the 400 mHz antenna at an antenna transmit rate of 100 mHz and the distance mode selected for use of the survey wheel on the cart. The scan menu was set with 512 samples, 16 bit format, 100 ns range or window, a dielectric constant of 8 (the default value), a scan rate of 100, and 50 scans per meter for the project area. In the gain menu, the gain was set to manual with a default value of 5. The gpr system was moved around the grid prior to the start of the survey to adjust the gain. If a location caused the trace wave to go off the screen, the gain was set to auto and then back to manual. The position was set to the manual mode with the offset value at the factory default and the surface display option set to zero. The filters were left at the default settings. With the setup completed, the run/stop button at the bottom of the display screen was selected and the collect mode was initiated. The gpr unit was moved across the grid and at the end of the traverse, the next file button was selected and data acquisition was halted. The gpr unit was placed at the start of the next line before saving the profile. Once the profile data was saved, the gpr unit was ready to collect the next profile line. The gpr data were recorded on a 512 mb compact flash card and transferred to a lap-top computer at the end of the survey.

6. DATA PROCESSING

Processing of geophysical data requires care and understanding of the various strategies and alternatives (Kvamme 2001:365; Music 1995; Neubauer et al. 1996). Drs. Roger Walker and Lewis Somers (Geoscan Research 2003) provide strategies, alternatives, and case studies on the use of several processing routines commonly used to process magnetic, resistance, and conductivity data in the GEOPLOT software. David et al. (2008:42-45) also provides a basic description of steps involved in the processing of magnetic, resistance, and ground penetrating radar data. Dr. Kenneth Kvamme (2001:365) provides a series of common steps used in computer processing of geophysical data:

> *Concatenation* of the data from individual survey grids into a single composite matrix;
>
> *Clipping and despiking* of extreme values (that may result, for example, from introduced pieces of iron in magnetic data);
>
> *Edge matching* of data values in adjacent grids through balancing of brightness and contrast (i.e., means and standard deviations);
>
> *Filtering* to emphasize high-frequency changes and smooth statistical noise in the data;
>
> *Contrast enhancement* through saturation of high and low values or histogram modification; and
>
> *Interpolation* to improve image continuity and interpretation.

It is also important to understand the reasons for data processing and display (David et al. 2008:45-49; Gaffney et al. 1991:11). They enhance the analyst’s ability to interpret the relatively huge data sets collected during the geophysical survey. The type of display can help the geophysical investigator present his interpretation of the data to the archeologist who will ultimately use the information to plan excavations or determine the archeological significance of the site from the geophysical data.

Processing Single Fluxgate Gradiometer System Magnetic Data

Upon completion of the magnetic survey with the single fluxgate gradiometer system, the data were processed in GEOPLOT (Tables 2 and 3). The grid data file was transformed into a composite file (Geoscan Research 2003:4/1-4/29) and a zero mean traverse was applied to remove any traverse discontinuities that may have occurred from operator handling or heading errors (Geoscan Research 2001:6/107-6/115). The magnetic data from the magnetic survey at the EFMO1 geophysical project area after the application of the zero mean traverse operation ranged from -103.6 nT to 120.4 nT with a mean of -0.13

nT and a standard deviation of 3.966 nT. The magnetic data from the magnetic survey at the EFMO2 geophysical project area after the application of the zero mean traverse operation ranged from -204.2 nT to 212.9 nT with a mean of 0.53 nT and a standard deviation of 27.278 nT. Upon completion of the zero mean traverse function, the data were interpolated by expanding the number of data points in the traverse direction and by reducing the number of data points in the sampling direction to provide a smoother appearance in the data set and to enhance the operation of the low pass filter (Geoscan Research 2001:6/53-6/56). This changed the original 8 x 1 data point matrix into a 4 x 4 data point matrix. The low pass filter was then applied over the entire data set to remove any high frequency, small scale spatial detail. This transformation may result in the improved visibility of larger, weak archeological features (Geoscan Research 2001:6/57-6/60). The data were then exported as an ASCII dat file and placed in the SURFER 8 contouring and 3d surface mapping program (Golden Software 2002). Image and contour maps of the single fluxgate gradiometer data were generated for the EFMO1 survey grid area (Figure 14) and the EFMO2 survey grid area (Figure 15).

Processing Dual Fluxgate Gradiometer System Magnetic Data

Upon completion of the magnetic survey with the dual fluxgate gradiometer system at the EFMO1 geophysical project area, the data were processed in ARCHAEOSURVEYOR (Table 4). The grid data file was assembled into a composite file (DW Consulting 2008:31-32). The raw magnetic data from the geophysical survey area ranged from -3000.0 nT to 1893.9 nT with a median of -3.50 nT and a standard deviation of 38.768 nT. The data was then clipped between -200 and 200 nT to eliminate the extreme outlying values, and a destripe operation was applied to remove any traverse discontinuities that may have occurred from operator handling or heading errors (DW Consulting 2008:9,60). The magnetic data from the geophysical survey area ranged from -200.0 nT to 200.0 nT with a median of -3.50 nT and a standard deviation of 6.710 nT after the application of the clip and the destripe operations. Upon completion of the destripe function, the data were interpolated by expanding the number of data points in the traverse direction and by reducing the number of data points in the sampling direction to provide a smoother appearance in the data set and to enhance the operation of the low pass filter (DW Consulting 2008:9,61). This changed the original 8 x 1 data point matrix into a 4 x 4 data point matrix. The low pass filter was then applied over the entire data set to remove any high frequency, small scale spatial detail (DW Consulting 2008:9,71). This transformation may result in the improved visibility of larger, weak archeological features. The data were then exported as an ASCII dat file (DW Consulting 2008:39) and placed in the SURFER 8 contouring and 3d surface mapping program (Golden Software 2002). Image and contour maps of the dual fluxgate gradiometer data were generated for the survey grid area at the EMFO1 survey grid area (Figure 16).

Processing Conductivity Data

The data were processed using the DAT38W software (Geonics 2002). After the transfer of the data and header files to the laptop computer, the files were automatically converted from the raw EM38 format to DAT38W format with the extension name of G38 (Geonics 2002:12-14). The data were then displayed as data profile lines (Geonics 2002:14-15). The individual EM38 data file was then converted to XYZ coordinate file in the SURFER 8 data format. To create the XYZ file, the orientation or direction of the survey line was selected in the DAT38W program along with the data type and format (Geonics 2002:20-23). The resulting XYZ data file was transfer to the SURFER 8 mapping software (Golden Software 2002). The conductivity data were reviewed and an image plot was generated in SURFER 8. To further process the conductivity data, it was transferred to GEOPLOT. The conductivity data were stripped of the X and Y coordinates and then the Z values (measurements) were imported into GEOPLOT (Tables 5 and 6) for further processing (Geoscan Research 2001). The resulting grid was formatted to form a composite file in GEOPLOT. The conductivity data from the conductivity survey at the EFMO1 survey area before processing ranged from 6.5 mS/m to 31.2 mS/m with a mean of 16.24 mS/m and a standard deviation of 2.732 mS/m. The conductivity data from the conductivity survey at the EFMO2 survey area before processing ranged from -115.1 mS/m to 42.0 mS/m with a mean of 14.91 mS/m and a standard deviation of 8.446 mS/m. An edge matching routine was applied to the conductivity data from the EFMO1 survey area to remove a grid edge discontinuity between two adjacent grid units in the southwest portion of the survey area (Geoscan Research 2001:6/45-6/47). The interpolation routine was applied to the two data set to arrange the data in an equally spaced 4 x 4 square matrix (Geoscan Research 2001:6/53-6/56). A high pass filter was then applied over the composite data sets. The high pass filter was used to remove low frequency, large scale spatial detail such as a slowing changing geological 'background' trend (Geoscan Research 2001:6/49-6/52). The data were exported as an ASCII *.dat file and placed in the SURFER 8 mapping program. Finally, image and contour maps of the conductivity data were generated for the EFMO1 survey grid area (Figure 17) and the EFMO2 survey grid area (Figure 18).

Processing Resistance Data

Upon completion of the resistance survey, the data were processed in GEOPLOT. The grid files were combined to form a composite file and further processed in GEOPLOT (Tables 7 and 8). The resistance data composite files from the EFMO1 survey grid area and the EFMO2 survey grid area were despiked to remove any erroneous measurements (Geoscan Research 2001:6/35-6/39). Despiking may be accomplished with the processing routine in GEOPLOT or manually by editing each individual grid file. The resistance data from the resistance survey at the EFMO1 survey grid area after the application of the despiking routine ranged from 31.2 ohms to 91.9 ohms with a mean of 44.27 ohms and a standard deviation of 9.176 ohms. The resistance data from the EFMO2 survey grid area after the routine ranged from 34.0 ohms to 82.0 ohms with a mean of 48.84 ohms and a standard deviation of 9.286 ohms. The interpolation routine was applied to the data set to arrange the data in an equally spaced 4 x 4 square matrix (Geoscan Research 2001:6/53-6/56). A high pass filter was then applied over the composite data set. The high pass filter was used to remove low frequency, large scale spatial detail such as a slowing changing geological ‘background’ trend (Geoscan Research 2001:6/49-6/52). The data were then exported as an ASCII *.dat file and placed in the SURFER 8 mapping program. Image and contour maps of the resistance data were generated for the EFMO1 survey grid area (Figure 19) and the EFMO2 survey grid area (Figure 20).

Processing Ground Penetrating Radar Data

The gpr radargram profile line data are imported into GPR-SLICE (Goodman 2005) for processing (Table 9). The first step in GPR-SLICE is to create a new survey project under the file menu. This step identifies the file name and folder locations. The next step is to create the information file. The number of profiles are entered, along with the file identifier name, .dzt for GSSI radargrams, the profile naming increment of 1, the first radargram name (generally this starts with 1), direction of profiling, x and y beginning and ending coordinates, units per marker (set to 1), the time window opening in nanoseconds (100 ns), samples per scan (512 s/scn), the number of scans per meter (these profiles were collected at 50 scans per meter), type of data (16 bit). Selecting the create info file button completes the information file for the project. The information file can be edited if necessary to correct profile lengths. The 16-bit GSSI radargrams are imported into the GPR-SLICE project folder for further processing. The 16-bit data are then converted to remove extraneous header information and to regain the data. During the conversion process, the signal is enhanced by applying gain to the radargrams. Once the conversion process is completed, the next step is to reverse the profile data. Since the radargrams were collected in the zigzag mode, every even line needs to be reversed. The reverse map button shows the radargrams that are going to be reversed. The next step is to insert navigation markers into the resample radargrams. The GSSI SIR 3000 and the artificial markers button are selected to apply markers based on the total number of scans in the radargram. The show markers button allows one to view an example of a radargram with the artificial markers in place. The next step is to create the time slices of the profile data (Conyers and Goodman 1997; Goodman et al. 1995). The program resamples the radargrams to a constant number of scans between the markers and collects the time slice information from the individual radargrams. The number of slices is set to 20 slices. The slice thickness is set to 30 to allow for adequate overlap between the slices. The offset value on the radargram where the first ground reflection occurs is viewed in the search 0 ns subroutine. This value is used to identify the first radargram sample at the ground surface. The end sample is 512. The offset value in entered in the samples to 0 ns box. The cut parameter is set to square amplitude with the cuts per mark set to 4. The slice/resample button is selected for processing the radargrams. The final step in the slice menu is to create the XYZ data file. The grid menu is entered next in the processing steps. The beginning and ending values for the x and y coordinate are entered. The help set button is selected to set the x search radius, y search radius and the blanking radius. The grid cell size is set to 0.1 and the search type is rectangular. The number of grids equal 20 for the number of slices, and the starting grid number is 1. The Kriging algorithm is utilized to estimate the interpolated data. The Varigram button is selected to set the Kriging range, nugget and sill parameters. The start gridding button is selected and the gridded dataset is created. In this menu, a low pass filter may be applied to the dataset to smooth noisy data in the time slices. At this point, one may view the time sliced radar data in the pixel map menu for the project area at the EFMO1 survey grid area (Figure 21). In addition, the original processed grid slices and the low pass filtered grid slices can be exported in the Surfer grid format. The surfer grid file is transformed into an image plot in Surfer. Generally, one time slice is selected for further display and analysis. Time slice 9 from 39 to 46 ns (Figure 22) is selected as the representative slice for further analysis of the gpr data at the EFMO1 project area. The gain may be readjusted for any time slice. This is done in the transforms submenu. The interpolations value is set to 5 and the interpolate grids routine is selected. The new interpolated grids are all normalized. The next step is to create the 3D dataset in the grid menu. The number of grids is now equal to 95 ((20-1)*5). The 3D database is created under the create 3D file routine. The 3D data may be displayed as a series of z slices in the creation of a 3D cube with a jpeg output for animating the 3D cube.

EFFIGY MOUNDS

7. DATA INTERPRETATIONS

Andrew David (1995:30) defines interpretation as a "holistic process and its outcome should represent the combined influence of several factors, being arrived at through consultation with others where necessary." Interpretation may be divided into two different types consisting of the geophysical interpretation of the data and the archaeological interpretation of the data. At a simplistic level, geophysical interpretation involves the identification of the factors causing changes in the geophysical data. Archeological interpretation takes the geophysical results and tries to apply cultural attributes or causes. In both cases, interpretation requires both experience with the operation of geophysical equipment, data processing, and archeological methodology; and knowledge of the geophysical techniques and properties, as well as known and expected archeology. Although there is variation between sites, several factors should be considered in the interpretation of the geophysical data. These may be divided between natural factors, such as geology, soil type, geomorphology, climate, surface conditions, topography, soil magnetic susceptibility, seasonality, and cultural factors including known and inferred archeology, landscape history, survey methodology, data treatment, modern interference, etc. (David 1995:30; David et al. 49). It should also be pointed out that refinements in the geophysical interpretations are dependent on the feedback from subsequent archeological investigations. The use of multiple instrument surveys provides the archeologist with very different sources of data that may provide complementary information for comparison of the nature and cause (i.e., natural or cultural) of a geophysical anomaly (Clay 2001). Each instrument responds primarily to a single physical property: magnetometry to soil magnetism, electromagnetic induction to soil conductivity, resistivity to soil resistance, and ground penetrating radar to dielectric properties of the soil to (Weymouth 1986:371).

Interpreting the Magnetic Data

Interpretation of the magnetic data (Bevan 1998:24) from the project requires a description of the buried archeological feature of object (e.g., its material, shape, depth, size, and orientation). The magnetic anomaly represents a local disturbance in the earth's magnetic field caused by a local change in the magnetic contract between buried archeological features, objects, and the surrounding soil matrix. Local increases or decreases over a very broad uniform magnetic surface would exhibit locally positive or negative anomalies (Breiner 1973:17). Magnetic anomalies tend to be highly variable in shape and amplitude. They are generally asymmetrical in nature due to the combined affects from several sources. To complicate matters further, a given anomaly may be produced from an infinite number of possible sources. Depth between the magnetometer and the magnetic source material also affect the shape of the apparent anomaly (Breiner 1973:18). As the distance between the magnetic sensor on the magnetometer and the source material increases, the expression of the anomaly becomes broader. Anomaly shape and amplitude are also affected by the relative amounts of permanent and induced magnetization, the direction of the magnetic field, and the amount of magnetic minerals (e.g., magnetite) present in the source compared to the adjacent soil matrix. The shape (e.g., narrow or broad) and orientation of the source material also affects the anomaly signature. Anomalies are often identified in terms of various arrays of dipoles or monopoles (Breiner 1973:18-19). A magnetic object in made of magnetic poles (North or positive and South or negative). A simple dipole anomaly contains the pair of opposite poles that relatively close together. A monopole anomaly is simply one end of a dipole anomaly and may be either positive or negative depending on the orientation of the object. The other end is too far away to have an affect on the magnetic field.

Magnetic anomalies of archeological objects tend to be approximately circular in contour outline. The circular contours are caused by small size of the objects. The shape of the object is seldom revealed in the contoured data. The depth of the archaeological object can be estimated by half-width rule procedure (Bevan 1998:23-24; Breiner 1973:31; Milsom 2003:67-70). The approximations are based on a model of a steel sphere with a mass of 1 kg buried at a depth of 1.0 m below the surface with the magnetic measurements made at an elevation of 0.3 m above the ground. The depth of a magnetic object is determined by the location of the contour value at half the distance between the peak positive value of the anomaly and the background value. With the fluxgate gradiometer, the contour value is half the peak value since the background value is approximately zero. The diameter of this contour (Bevan 1998:Fig. B26) is measured and used in the depth formula where **depth = diameter – 0.3 m** (Note: The constant of 0.3 m is the height of the bottom fluxgate sensor above the ground in the Geoscan Research FM36 were I carry the instrument during data acquisition. This value needs to be adjusted for each individual that carries the instrument.). The mass in kilograms of the object (Bevan 1998:24, Fig. B26) is estimated by the following formula: **mass = (peak value - background value) * (diameter)^3/60**. It is likely that the depth and mass estimates are too large rather than too small, since they are based on a compact spherical object made of iron. Archeological features are seldom compact but spread out in a line or lens. Both mass and depth estimates will be too large. The archaeological material may be composed of something other than iron such as fired earth or volcanic rock. Such materials are not usually distinguishable from the magnetic data collected during the survey (Bevan 1998:24). The depth and mass of features comprised of fired earth, like that found in kilns, fireplaces, or furnaces could be off by 100 times the mass of iron. If the archeological feature were comprised of bricks (e.g., brick wall, foundation, or chimney), estimates could be off by more than a 1000 times that of iron. The location of the center of the object can also be determined by drawing a line connecting the peak positive and peak negative values. The rule of thumb is that the center of the object is located approximately one third to one half of the way along the line from the peak positive value for the anomaly. One should also be cautious of geophysical anomalies that extend in the direction of the traverses since these may represent operator-induced errors. The magnetic gradient anomalies may be classified as three different types: linear, 2) dipole, and 3) monopole.

The first step in interpreting the magnetic anomalies from the project area is to identify areas of high magnetic contrast and, especially, the positive magnetic anomalies or the North pole of the dipole. Numerous magnetic anomalies from the single fluxgate gradiometer survey occur across the two project areas. At the EFMO1 project area, there is a light scatter of magnetic anomalies suggesting the locations of buried ferrous objects (Figure 23). One extremely strong anomaly near N24/E28 may represent the buried remains of a steel fence post. In addition to the dipole and monopole magnetic anomalies, which appear to be associated with buried ferrous object, there are a number of linear anomalies. Two nearly parallel and very weak anomalies may represent an access road to this potion of the landscape. The linear anomalies correspond to the ruts noted during the survey. The two bear and three conical mound group identified by T. H. Lewis appear as faint positive magnetic anomalies. The smaller of the two bears is located in the area of the two linear magnetic anomalies associated with the road ruts. In addition to the faint outlines of the two bears and the three conical mounds, there are at least four more circular magnetic anomalies that may suggest the present of other conical mounds in the vicinity of the mound group identified by Lewis. At EFMO2, the magnetic data indicate the presence of more ferrous materials that at EFMO1. The two mounds at EFMO2 are identified by contrasts in the magnetic data that differ greatly from the background magnetic field (Figure 24). In addition, the bird effigy contains a substantial trash dump of ferrous materials on its eastern side. The excavated trenches in both mounds are represented by linear magnetic lows.

The dual fluxgate gradiometer data from the EFMO1 project area is similar to the magnetic data from the single fluxgate gradiometer survey (Figure 25) The linear ruts are identified as magnetic lows. The bear and conical mound groups identified by T. H. Lewis appears as faint positive magnetic anomalies. The smaller of the two bears is located in the area of the two linear magnetic anomalies associated with the road ruts. In addition to the faint outlines of the two bears and the three conical mounds, there are at least four more circular magnetic anomalies that may suggest the present of other conical mounds in the vicinity of the mound group identified by Lewis. Other linear anomalies appear to indicate geological trends at the foot and toe of the side slope in both data sets. The major difference between the single and the dual fluxgate gradiometer data sets is result of the sensor separation between the two instruments. If the gradient change is slight, the single fluxgate gradiometer does not reflect the change over the shorter 0.5 meter distance as much as the change over the meter distance. The dual fluxgate gradiometer tends to emphasis weaker changes enhancing the contrasts between the high and low values of the magnetic anomalies.

Interpreting the Conductivity Data

Interpretation of the conductivity data results in the identification of lateral changes in the soil matrix. The conductivity data may be divided into three classes of anomalies including linear anomalies, point anomalies, and broad anomalous areas. Linear anomalies may represent foundations of buildings, trenches, buried utility lines, paths, trails, or roads that are longer that they are wide. Point anomalies tend to represent buried objects or vertical structures such as cisterns, wells, or storage pits. Occasionally, these anomalies may have negative values resulting from the saturation of the receiving coil by the overwhelming conductive metal response of buried metals to the generated electromagnetic field. Comparisons between these negative conductivity anomalies and the magnetic anomalies can elucidate the nature of the buried object. If the magnetic and conductivity point anomalies coincide, it is assumed that the buried object is made from ferrous material. The presence of a magnetic anomaly and the lack of a corresponding conductivity anomaly suggest that the magnetic anomaly is composed of non-metallic material such as fired clay typically found in fire related features (i.e., fire hearths or pits, concentrated areas of ceramics, or bricks). The presence of a negative conductivity anomaly and the absence of a corresponding magnetic anomaly strongly suggest that the buried object is some type of non-ferrous metal (e.g., brass, copper, lead, etc.). Broad anomalous areas typically represent large areas of soil disturbances or compaction often found associated with gardens, basements or cellars, parking pads, compacted dirt floors, or areas of concrete or asphalt.

At the EFMO1 geophysical project area, there are a few negative value conductivity anomalies spread across the survey area (Figure 26). Several of these coincide with magnetic anomalies suggesting that the use of these two complementary data sets helps in the identification of the buried ferrous metal objects. In addition, the density of these point conductivity anomalies is much less than the associated magnetic dipole anomalies. In locations where the conductivity and magnetic anomalies coincide, the object causing the anomalous measurement is probably ferrous metal. In the cases where a magnetic anomaly is present and a conductivity anomaly is absent, The buried material may be fire-related materials such as brick or other burned materials. If the conductivity anomaly is not associated with a magnetic anomaly, the buried object may be non-ferrous metal. A large cluster of conductivity anomalies appear represent a soil disturbance along the bench where the ruts are located. The road ruts and other linear conductivity anomalies are represented as weak conductivity anomalies. The bear and conical mound groups identified by T. H. Lewis appears as faint positive conductivity anomalies. The smaller of the two bears is located in the area of the two linear conductivity anomalies associated with the road ruts. In addition to the faint outlines of the two bears and the three conical mounds, there are at least four more circular conductivity anomalies that may suggest the present of other conical mounds in the vicinity of the mound group identified by Lewis. The other linear anomalies appear to represent geological contrasts that were also noted in the magnetic data sets.

At EFMO2, there are a few negative value conductivity anomalies spread across the survey area; however, there are three major concentrations coinciding with the metal artifacts on the surface, which represent trash dumps locations within the project area (Figure 27). Several of these coincide with magnetic anomalies suggesting that the use of these two complementary data sets helps in the identification of the buried ferrous metal objects. In addition, the density of these point conductivity anomalies is much less than the associated magnetic dipole anomalies. In locations where the conductivity and magnetic anomalies coincide, the object causing the anomalous measurement is probably ferrous metal. The presence of a magnetic anomaly and the lack of a corresponding conductivity anomaly suggest that the magnetic anomaly is composed of non-metallic material such as fired clay typically found in fire related features (i.e., fire hearths or pits, concentrated areas of ceramics, or bricks). The presence of a negative conductivity anomaly and the absence of a corresponding magnetic anomaly strongly suggest that the buried object is some type of non-ferrous metal (e.g., brass, copper, lead, etc.). The two mounds noted in the project area are outlined as faint positive conductivity anomalies. The trenches within the mounds are represented by linear conductivity anomalies that are slightly higher in conductivity that the surrounding mound fill and general background conductivity levels.

Interpreting the Resistance Data

Interpretation of the resistivity data results in the identification of lateral changes in the soil. Since the array parameters are kept constant through out the survey, the resulting resistance values varies with changes in the subsurface sediments/soil matrix and buried archeological resources. For each probe separation, the depth penetration is approximately the same as the distance between the current and potential probe on the mobile array frame, which was 0.5 meters. The resistance measurement for each point represents the average value for the hemispheric volume of soil with the same radius. If the soil below the survey area was uniform, the resistivity would be constant throughout the area. Changes in soil characteristics (e.g., texture, structure, moisture, compactness, etc.) and the composition of archeological features result in differences in the resistances across the surveyed grid. Large general trends reflect changes in the site's geology whereas small changes may reflect archeological features. An advantage to the resistance survey and its interpretation is its usefulness in areas that have high concentrations of metal objects such as the three project areas in this study.

The resistance data from the EMFO1 geophysical survey area illustrates a number of resistance anomalies previously identified in the dual and single magnetic, and conductivity data sets from the project area (Figure 28). The two bears and the three conical mounds that were documented by T. H. Lewis are represented in the resistance data as very faint resistance highs. The square shaped resistance anomaly in the northeast corner of the survey grids may represent a historic cabin dating to the late 1800s. The resistance anomaly consists of a square shaped anomaly of slightly higher resistance than the surrounding area. It also appears to have internal divisions. The areas identified as possible conical mounds area also represented as a ring of slightly higher resistance values from the surrounding area. The two linear anomalies associated with the road tracks, appear as resistance lows. A large area in the northern part of the resistance survey area indicates that there has been substantial disturbance of the landscape.

The resistance data from the EMFO2 geophysical survey area illustrates a number of resistance anomalies previously identified in the dual and single magnetic, and conductivity data sets from the project area (Figure 29). The conical mound is represented in the resistance data by a circular ring of low resistance values while the interior of the mound contains substantially higher resistance values. The effigy mound is not as well defined as the smaller conical mound. The edge of the mound in some locations consists of a linear resistance low outlining the mound. The excavated backdirt from the interior of the mound is piled along the sides of the body and underneath the wings of the effigy. The trenches into the two mounds appear as linear resistance lows. The deep circular excavation on the inside of the effigy mound contains lower resistance values than the surrounding mound fill.

Interpreting the Ground Penetrating Radar Data

Analysis and interpretation of the gpr data may be conducted in several different ways. The individual radargrams for each profile line may be analyzed for hyperbolic reflections. The radargrams may be combined and processed to provide planar time slices of the data. The time slices may also be combined to form 3D cubes of the gpr data. The majority of the gpr radargrams show numerous small reflections along any given profile. Most of the analysis of the gpr data is done with the 3D display while moving through the numerous time slices, but in order to provide a graphic representation of the anomalous areas, an individual time slice was selected.

The ground penetrating radar data from the EFMO1 geophysical project area, illustrated by the time slice 9 layer (Figure 30), contains a number of high amplitude strength reflections across the yard. The two road ruts are identified as high amplitude reflections. In the northeast corner of the project grid, the rectangular or square-shaped gpr anomaly consists of a high amplitude reflection outline enclosing lower interior amplitude reflections. The gpr anomaly has been potentially identified as a historic cabin location. The mound group identified and documented by T. H. Lewis consists of higher amplitude reflections outlining the two bear effigies and the three conical mounds. In addition to these gpr anomalies associated with the documented mound group, there are four locations within the survey area that contain similar contracts in the gpr data that were found in the conical mounds identified in the documented mound group. It is possible that these gpr anomalies represent the locations of destroyed mounds that were not detected by Lewis during his documentation of the Nezekaw Terrace Mound Group in 1892.

Combined Geophysical Data Set Interpretations

A different way of looking at the geophysical data collected during the investigations of the survey area at proposed interpretative heirloom garden location is to combine the complementary data sets into one display. A number of the different geophysical anomalies overlap suggesting a strong correlation between the geophysical data and the buried archeological features (Ambrose 2005). A number of the different geophysical anomalies overlap suggesting a strong correlation between the geophysical data and the buried archeological features (Ambrose 2005; Kvamme 2007:345-374). These areas of overlap would be considered areas of high probability for ground truthing and the investigations of buried archeological resources. While these correlations are important, individual isolated occurrences also need ground truthing in order to determine their unique nature as well. The locations of the possible mound remnants, historic structures and trash dumps, roads, and artifact locations and concentrations are present in the geophysical data from the EMFO1 geophysical project area (Figure 31). Complementary data from the geophysical survey efforts at the EMFO1 geophysical project area in the three residential lots also indicate the locations of two mounds, trash dumps, mound disturbances, and adjacent roadways (Figure 32).

EFFIGY MOUNDS

8. CONCLUSIONS AND RECOMMENDATIONS

During the week of June 8-14, 2008, Midwest Archeological Center staff, University of Nebraska-Lincoln graduate student, and Volunteer-In-Park participants conducted geophysical investigations at the Nezekaw Terrace Mound Group, 13AM82, in Effigy Mounds National Monument in Allamakee County, Iowa. The geophysical investigations were part of the anthropology graduate Masters Thesis study of Jim Lindsay at the University of Nebraska-Lincoln. The geophysical investigations included magnetic surveys with a single and dual fluxgate gradiometer systems, a resistance survey with a resistance meter and twin probe array, a conductivity survey with a ground conductivity meter, and a ground penetrating radar survey with a ground penetrating radar cart system and 400 mHz antenna at the EMFO1 geophysical project area within Site 13AM82. The geophysical investigations also included a magnetic survey with a single fluxgate gradiometer system, a conductivity survey with a conductivity meter, and a resistance survey with a resistance meter and twin probe array at the EMFO2 geophysical project area within Site 13AM82. The total geophysical survey area for both project locations was 3,721 m^2 or 0.92 acres with the geophysical instruments.

The surveys resulted in the identification of numerous subsurface anomalies. The magnetic gradient, resistance, conductivity, and ground penetrating radar data collected at the site provided information of the physical properties (magnetic, soil resistance, and ground-penetrating radar reflection properties) of the subsurface materials. Standard methodology for conducting geophysical investigations was used with standard 20-meter by 20-meter grid sizes where feasible. The results of the geophysical survey indicated the presence of mound remnants associated with the bear and conical mound group documented by T. H. Lewis in 1892 and re-investigated by E. Orr in 1926, additional possible conical mound remnants, road ruts, a historic cabin location, and disturbed areas at EMFO1. The two mounds at EMFO2 were identified in the geophysical data, as well as trenching activities or disturbances to the two mounds, adjacent road beds and historic trash dumps within the geophysical project area. Numerous magnetic and conductivity anomalies indicated the presence of buried ferrous and non-ferrous objects across the two project areas. The resistance, ground penetrating radar, magnetic, and conductivity anomalies represented the outlines of buried mound remnants at EMFO1, while the integrity of the two mounds at EMFO2 were documented as a result of the magnetic, resistance, and conductivity surveys within the survey area.

The geophysical results from the two project areas within Site 13AM82 raises as many questions as they answer. At the EMFO1 geophysical project area, the remnants of the two bears and three conical mounds documented by T. H. Lewis in his 1892 field investigations have been identified in the geophysical data collected at the site. It took a combined analysis of the geophysical data along with recent LiDAR data and historic aerial photographs (Jim Lindsay 2009, personal communications) to identify the subtle contrasts between the geophysical anomalies representing the outlines of the mounds and the background physical properties of the undisturbed and disturbed soils surrounding the mound outlines. In addition to the documented mound group, at least four geophysical anomaly contrasts suggest the existence of other conical mounds that were not documented by Lewis. Ground truthing of the geophysical anomalies identified at EMFO1 is needed to determine the nature of the buried and remnant archeological features. These activities should also include the geomorphic techniques originally conducted in the Iowa State University Ph.D. dissertation study of the mounds within Effigy Mounds National Monument by Roger Parsons (1962) and the more recent magnetic susceptibility techniques developed for environmental and archeological investigations (Dalan 2008; Thompson and Oldfield 1986:83-87).

The results of the geophysical investigations at the EMFO2 geophysical project area posed additional research questions concerning the nature of the larger mound, which is tentatively identified as a bird effigy (Jim Lindsay 2008, personal communications). The shape of the suspected effigy mound is an oddity within the general bird effigy forms found at Effigy Mounds National Monument (Mallam 1976:104). The disturbance to the mound caused by the non-professional excavations of the mound may have an impact on the present interpretation of the mound as a bird effigy. The short stubby “wings” off the body of the mound along with the raised tail suggest the bird effigy form for the mound; however, the amount of excavation or disturbance to the mound may have altered its original shape. The removal of mound fill from the body of the mound was piled along the edges of the lower part of the body of the mound. It is also possible that the wings were deposited during the excavation of the mound to form drainage away from the mound. The presence of the trash dump at the mound may offer an alternative to the mound form. The question that the present research raises is the possibility that the mound was originally conical shaped and modifications to the interior of the mound has resulted in the bird effigy like shape of the mound. One alternative hypothesis to the aboriginal effigy shape would be the construction of a historic cabin within the body of a conical mound resulting in the deep excavations noted during the survey and the presence of a large trash dump on the north side of the mound along the historic private road. In Orr’s 1926 map of the Nezekaw Terrace Mound Group compiled form Lewis’ field notes and sketches, there are two mounds located to the north of the bear effigies and conical mounds platted by Lewis. A private road is located on the south side of the two mounds, which was identified during the present geophysical investigations (Jim Lindsay, personal communications 2008). The question is whether these two conical mounds represented by Orr are the two mounds identified in the geophysical survey of the EFMO2 geophysical project area. Additional ground truthing is needed to resolve the current dilemma as to the nature of the large mound and association of the two conical mounds with the bear effigies and three conical mounds platted by Lewis and depicted in Orr’s 1926 drawing.

Finally, refinement of the archeological and geophysical interpretation of the survey data is dependent on the feedback of the archeological investigations following geophysical survey (David 1995:30). Should additional archeological investigations occur at the site investigated during this project, the project archeologist is encouraged to share additional survey and excavation data with the geophysical investigator for incorporation into the investigator's accumulated experiences with archeological problems. Throughout the entire geophysical and archeological investigations, communication between the geophysicist and the archeologist is essential for successful completion of the archeological investigations. It is also important for the investigators to disseminate the results of the geophysical survey and archeological investigations to the general public. It is through their support in funds and labor that we continue to make contributions to the application of geophysical techniques to the field of archeology.

This report has provided a cursory review and analysis of the geophysical data collected during the geophysical investigations of the Nezekaw Terrace Mound Group (Site 13AM82) at Effigy Mounds National Monument. The geophysical techniques applied to the investigations at Site 13AM82 have proven successful in the identification of remnant mound outlines in the present geophysical project areas. Other geophysical investigations at the park have also proven successful in the identification of the mounds and subsurface features within the mounds. The geophysical techniques combined with aerial photography and LiDAR have the potential to identify the subsurface remnants of mounds across the park. This information will be used by the Midwest Archeological Center and the Effigy Mounds National Monument staffs to guide further archeological inquiry into the nature of the archeological resources at the site and help direct future National Park Service geophysical surveys and archeological excavations at other sites within the boundary of Effigy Mounds National Monument.

EFFIGY MOUNDS

REFERENCES CITED

Ambrose, Heather M.
2005 *Quantitative Integration and Three-dimensional Visualization of Multi-archaeological geophysics Survey*. ProQuest Information and Learning Company, Ann Arbor, Michigan.

Annan, A. P.
2005 Ground-Penetrating Radar. In *Near-Surface Geophysics*, edited by Dwain K. Butler, pp. 357-438. Society of Exploration Geophysicists, Tulsa, Oklahoma.

Aspinall, Arnold, Chris Gaffney, and Armin Schmidt
2008 *Magnetometry for Archaeologists*. AltaMira Press, Lanham, Maryland.

Bartington Instruments
2007 *Operation Manual for Grad 601 Single Axis Magnetic Gradiometer*. OM1800. Bartington Instruments, Oxford, England.

Beaubien, Paul L.
1952 Preliminary Report of the Archeological Investigations at Effigy Mounds National Monument 1950. Ms. on file, Effigy Mounds National Monument, McGregor, Iowa.

Benn, David W., and Scott Stadler
2004 *Effigy Mounds National Monument Archeological Overview and Assessment*. BCA #1087. Bear Creek Archaeology Inc., Cresco, Iowa.

Bevan, Bruce W.
1983 Electromagnetics for Mapping Buried Features. *Journal of Field Archaeology* 10(1):47-54.

1991 The Search for Graves. *Geophysics* 56(9):1310-1319.

1998 *Geophysical Exploration for Archaeology: An Introduction to Geophysical Exploration*. Special Report No. 1. Midwest Archeological Center, Lincoln, Nebraska.

Breiner, Sheldon
1973 *Applications Manual for Portable Magnetometers*. GeoMetrics, Sunnyvale, California.

1992 Magnetics: Applications for Portable Magnetometers. In *Practical Geophysics II for the Exploration Geologist*, compiled by Richard Van Blaricom, pp. 313-381, Northwest Mining Association, Spokane, Washington.

EFFIGY MOUNDS

Brown, Lauren
1985 *The Audubon Society Nature Guides: Grasslands*. Alfred A. Knopf, New York.
Burger, H. Robert

1992 *Exploration Geophysics of the Shallow Subsurface*. Prentice Hall PTR, Englewood Cliffs, New Jersey.

Carr, Christopher
1982 *Handbook on Soil Resistivity Surveying: Interpretation of Data from Earthen Archeological Sites*. Research Series, Volume 2. Center for American Archeology Press, Evanston, Illinois.

Clark, Anthony
2000 *Seeing Beneath the Soil: Prospecting Methods in Archaeology*. Reprint. Routledge, London. Originally published in 1990 by B. T. Batsford, Ltd., London.

Clay , R. Berle
2001 Complementary Geophysical Survey Techniques: Why Two Ways are always Better than One. *Southeastern Archaeology* 20(1):31-43.

2006 Conductivity Survey: A Survival Manual. In *Remote Sensing in Archaeology: An Explicitly North American Perspective* by Jay K. Johnson, pp. 79-107. University of Alabama Press, Tuscaloosa.

Conyers, Lawrence B.
2004 *Ground-Penetrating Radar for Archaeology*. AltaMira Press, Walnut Creek, California.

2006 Ground-Penetrating Radar. In *Remote Sensing in Archaeology: An Explicitly North American Perspective*, edited by Jay K. Johnson, pp. 131-159. University of Alabama Press, Tuscaloosa.

2007 Ground-penetrating Radar for Archaeological Mapping. In *Remote Sensing in Archaeology*, edited by James Wiseman and Farouk El-Baz, pp. 329-344. Springer, New York.

Conyers, Lawrence B., and Dean Goodman
1997 *Ground-Penetrating Radar: An Introduction for Archaeologists*. AltaMira Press, Walnut Creek, California.

Conyers, Lawrence B., and Jeffrey E. Lucius
1996 Velocity Analysis in Archaeological Ground-penetrating Radar Studies. *Archaeological Prospection* 3(1):25-38.

Dalan, Rinita A.

1995 Geophysical Surveys for Archaeological Research: Electromagnetic Conductivity Surveys. Ms. on file, Midwest Archeological Center, National Park Service, Lincoln, Nebraska. <http://www.cast.uark.edu/nadag/EducationalMaterials/EM/Dalan1.pdf>.

2008 A Review of the Role of Magnetic Susceptibility in Archaeogeophysical Studies in the USA: Recent Developments and Prospects. *Archaeological Prospection* (15(1):1-31.

Davenport, G. Clark

2001 *Where is it? Searching for Buried Bodies & Hidden Evidence*. SportWork, Church Hill, Maryland.

David, Andrew

1995 *Geophysical Survey in Archaeological Field Evaluation*. Research & Professional Services Guidelines No. 1. Ancient Monuments Laboratory, English Heritage, London.

2001 Overview—The Role and Practice of Archaeological Prospection. In *Handbook of Archaeological Sciences*, edited by D. R. Brothwell and A. M. Pollard, pp. 521-527. John Wiley & Sons, Ltd., Chichester, England.

David, Andrew, Neil Linford, and Paul Linford

2008 *Geophysical Survey in Archaeological Field Evaluation*. Second Edition. Research & Professional Services Guidelines No. 1. Ancient Monuments Laboratory, English Heritage, London.

De Vore, Steven L.

2008 Geophysical Investigations at Effigy Mounds National Monument, Allamakee County, Iowa (June 8-14). Trip Report on file, Midwest Archeological Center, Lincoln, Nebraska.

Dice, Lee R.

1943 *The Biotic Provinces of North America*. University of Michigan Press, Ann Arbor.

Dobrin, Milton B., and Carl H. Savit

1988 *Introduction to Geophysical Prospecting*. Fourth Edition. McGraw-Hill Book Company, New York.

DW Consulting

2008 *ArchaeoSurveyor User Manual*. Program Version 2.3.0X, Issue 2. DW Consulting, Barneveld, The Netherlands.

Fenneman, Nevin M.
1938 *Physiography of Eastern United States*. McGraw-Hill Book Company, New York.

Fitterman, David V., and Victor F. Labson
2005 Electromagnetic Induction Methods for Environmental Problems. In *Near-Surface Geophysics*, edited by Dwain K. Butler, pp. 301-355. Society of Exploration Geophysicists, Tulsa, Oklahoma.

Gaffney, Chris, and John Gater
2003 *Revealing the Buried Past: Geophysics for Archaeologists*. Tempus Publishing, Stroud, Great Britain.

Gaffney, Chris, John Gater, and Sue Ovenden
1991 *The Use of Geophysical Techniques in Archaeological Evaluations*. Technical Paper Number 9. Institute of Field Archaeologists, University of Birmingham, Birmingham, England.

2002 *The Use of Geophysical Techniques in Archaeological Evaluations*. Paper No. 6. Institute of Field Archaeologists, University of Reading, Reading, England.

Geonics
1992 *EM38 Ground Conductivity Meter Operating Manual for EM38 Models with Digital Readout*. Geonics Limited, Mississauga, Ontario, Canada.

1998 DL720/38 Data Logging System Operating Instructions for EM38 Ground Conductivity Meter with Polycorder Series 720, Version 3.40. Geonics Limited, Mississauga, Ontario, Canada.

2002 *DAT38W Version 1.10 Computer Program Manual (Survey Data Reduction Manual)*. Geonics Limited, Mississauga, Canada.

Geoscan Research
1987 *Fluxgate Gradiometer FM9 FM18 FM36 Instruction Manual, Version 1.0*. Geoscan Research, Bradford, England.

1996 *Resistance Meter RM15 Instruction Manual, Version 2.4*. Geoscan Research, Bradford, England.

2001 *Geoplot Version 3.00 for Windows Instruction Manual, Version 1.6*. Geoscan Research, Bradford, England.

2003 *Geoplot Version 3.00 for Windows Instruction Manual, Version 1.6*. Geoscan Research, Bradford, England.

2006 *Fluxgate Gradiometer FM256 Instruction Manual, Version 1.7*. Geoscan Research, Bradford, England.

Golden Software
2002 *Surfer 8 User's Guide: Contouring and 3D Surface Mapping for Scientists and Engineers*. Golden Software, Golden, Colorado.

Goodman, Dean
2005 *GPR-SLICE v 5.0 Ground Penetrating Radar Imaging Software Quickstart Introduction*. Geophysical Archaeometry Laboratory, Woodland Hills, California.

Goodman, D., Y. Nishimura, and J. D. Rogers
1995 GPR Time Slices in Archaeological Prospection. *Archaeological Prospection* 2(2):85-89.

Goodman, Dean, Kent Schneider, Salvatore Piro, Yasushi Nishimura, and Agamennon G. Pantel
2007 Ground Penetrating Radar Advances in Subsurface Imaging for Archaeology. In *Remote Sensing in Archaeology*, edited by James Wiseman and Farouk El-Baz, pp. 375-394. Springer, New York.

GSSI
2003 *TerraSIRch SIR System-3000 User's Manual*. Geophysical Survey Systems, Inc., North Salem, New Hampshire.

Hallof, Philip G.
1992 Electrical: IP and Resistivity: Grounded Electrical Methods in Geophysical Exploration. In *Practical Geophysics II for the Exploration Geologist*, compiled by Richard Van Blaricom, pp. 313-381, Northwest Mining Association, Spokane, Washington.

Hansen, R. O., Louis Racic, and V. J. S. Grauch
2005 Magnetic Methods in Near-Surface Geophysics. In *Near-Surface Geophysics*, edited by Dwain K. Butler, pp. 151-175. Society of Exploration Geophysicists, Tulsa, Oklahoma.

Heimmer, Don H. and Steven L. De Vore
1995 *Near-Surface, High Resolution Geophysical Methods for Cultural Resource Management and Archeological Investigations.* Revised edition. National Park Service, Denver, Colorado.

2000 Near-Surface, High Resolution Geophysical Methods for Cultural Resource Management and Archaeological Investigations. In *Science and Technology in Historic Preservation*, edited by Ray A. Williamson and Paul R. Nickens, pp. 53-73. Advances in Archaeological and Museum Science, Volume 4. Kluwer Academic/Plenum Publishers, New York.

HRA Gray & Pape

2003 *Figures on the Landscape: Effigy Mounds National Monument Historic Resource Study*. HRA Gray & Pape LLC, Seattle, Washington.

Hunt, Charles B.

1967 Physiography of the United State. W. H. Freeman and Company, San Francisco.

Klien, Jan, and Jules J. Lajoie

1992 Electromagnetics: Electromagnetic Prospecting for Minerals. In *Practical Geophysics II for the Exploration Geologist*, compiled by Richard Van Blaricom, pp. 313-381, Northwest Mining Association, Spokane, Washington.

Kvamme, Kenneth L.

2001 Current Practices in Archaeogeophysics: Magnetics, Resistivity, Conductivity, and Ground-Penetrating Radar. In *Earth Sciences and Archaeology*, edited by Paul Goldberg, Vance T. Holliday, and C. Reid Ferring, pp. 353-384. Kluwer Academic/Plenum Publishers, New York.

2003 Geophysical Surveys as Landscape Archaeology. *American Antiquity* 68(3):435-457.

2005 Terrestrial Remote Sensing in Archaeology. In *Handbook of Archaeological Methods*, edited by Herbert D. G. Maschner and Christopher Chippindale, pp. 423-477. AltaMira Press, Lanham, Maryland.

2006a Magnetometry: Nature's Gift to Archaeology. In *Remote Sensing in Archaeology: An Explicitly North American Perspective*, edited by Jay K. Johnson, pp. 205-233. University of Alabama Press, Tuscaloosa.

2006bData Processing and Presentation. In *Remote Sensing in Archaeology: An Explicitly North American Perspective*, edited by Jay K. Johnson, pp. 235-250. University of Alabama Press, Tuscaloosa.

2007 Integrating Multiple Geophysical Datasets. In *Remote Sensing in Archaeology*, edited by James Wiseman and Farouk El-Baz, pp. 345-374. Springer, New York.

Kvamme, Kenneth L., Jay K. Johnson, and Bryan S. Haley
2006 Multiple Methods Surveys: Case Studies. In *Remote Sensing in Archaeology: An Explicitly North American Perspective*, edited by Jay K. Johnson, pp. 251-267. University of Alabama Press, Tuscaloosa.

Lenzendorf, Dennis
2000 *Effigy Mounds: A Guide to Effigy Mounds National Monument*. Eastern National, Fort Washington, Pennsylvania.

Lowrie, William
1997 *Fundamentals of Geophysics*. Cambridge University Press, Cambridge, United Kingdom.

Mallam, R. Clark
1976 *The Iowa Effigy Mound Manifestation: An Interpretive Model*. Report 9. Office of the State Archaeologist, Iowa City, Iowa.

McNeill, J. Duncan
1980a *Electrical Conductivity of Soils and Rocks*. Technical Note TN-5. Geonics Limited, Mississauga, Canada.

1980b *Electromagnetic Terrain Conductivity Measurements at Low Induction Numbers*. Technical Note TN-6. Geonics Limited, Mississauga, Canada.

Milsom, John
2003 *Field Geophysics*. Third Edition. John Wiley & Sons, Chichester, United Kingdom.

Music, B.
1995 On-Site Prospection in Slovenia: The Case of Rodik. *Archaeological Computing Newsletter* 43:6-15.

Mussett, Alan E., and M. Aftab Khan
2000 *Looking into the Earth: An Introduction to Geological Geophysics*. Cambridge University Press, Cambridge, United Kingdom.

Neubauer, W., P. Melichar, and A. Eder-Hinterleitner
1996 Collection, Visualization, and Simulation of Magnetic Prospection Data. In *Interfacing the Past: Computer Applications and Quantitative Methods in Archaeology, CAA95, Volume 1*, edited by H. Kamermans and K. Fennema, pp. 121-129. Analecta Praehistorica Leidensia No. 28. University of Leiden, Leiden, The Netherlands.

Nishimura, Y.
2001 Geophysical Prospection in Archaeology. In *Handbook of Archaeological Sciences*, edited by D. R. Brothwell and A. M. Pollard, pp. 543-553. John Wiley & Sons, Ltd., Chichester, England.

O'Bright, Jill York
1989 *The Perpetual March: An Administrative History of Effigy Mounds National Monument*. National Park Service, Omaha, Nebraska.

Orr, Ellison
1939 Sundry Archaeological Papers and Memoranda, Vol. XII: Iowa Archaeological Reports 1934-1939. In *Archives of Archaeology*, edited by David Baerreis, Society for American Archaeology Microcard Series 20, University of Wisconsin Press, Madison.

Parsons, Roger B.
1962 Indian Mounds of Northeast Iowa as Soil Genesis Benchmarks. *Journal of the Iowa Archeological Society* 12(2):1-70.

Peddie, Norman W.
1992 *The Magnetic Field in the United States, 1990, Total Intensity Chart*. U.S. Geological Survey Geophysical Investigations Map GP-1002-F. U.S. Geological Survey, Reston, Virginia.

Peddie, Norman W., and Audronis K. Zundie
1988 *The Magnetic Field in the United States, 1985, Inclination Chart*. U.S. Geological Survey Geophysical Investigations Map GP-986-I. U.S. Geological Survey, Reston, Virginia

Robinson, Edwin S., and Cahit Çoruh
1988 *Basic Exploration Geophysics*. John Wiley & Sons, New York.

Roosevelt, A. C.
2007 Geophysical Archaeology in the Lower Amazon: A Research Strategy. In *Remote Sensing in Archaeology*, edited by James Wiseman and Farouk El-Baz, pp. 443-4475. Springer, New York.

Scollar, I., A. Tabbagh, A. Hesse, and I Herzog
1990 *Archaeological Prospection and Remote Sensing*. Topics In Remote Sensing 2. Cambridge University Press, Cambridge, England.

Sharma, Prem V.
1997 *Environmental and Engineering Geophysics*. Cambridge University Press, Cambridge, United Kingdom.

Shelford, Victor E.
1974 *The Ecology of North America*. University of Illinois Press, Urbana.

Sheriff, Robert E.
1973 *Encyclopedic Dictionary of Exploration Geophysics*. Society of Exploration Geophysicists, Tulsa, Oklahoma.

Somers, Lewis
2006 Resistivity Survey. In *Remote Sensing in Archaeology: An Explicitly North American Perspective*, edited by Jay K. Johnson, pp. 109-129. University of Alabama Press, Tuscaloosa.

Stadler, Scott, and Robert Nickel
1999 South Unit Access Project, Effigy Mounds National Monument, October 29, 1999. Trip Report on file, Midwest Archeological Center, National Park Service, Lincoln, Nebraska.

Sutton, Ann, and Myron Sutton
1985 *The Audubon Society Nature Guides: Eastern Forests*. Alfred A. Knopf, New York.

Telford, W. M., L. P. Geldart, and R. E. Sheriff
1990 *Applied Geophysics*. Second Edition. Cambridge University Press, Cambridge, United Kingdom.

Thompson, Roy, and Frank Oldfield
1986 *Environmental Magnetism*. Allen & Unwin, London, United Kingdom.

Trewartha, Glenn T., and Lyle H. Horn
1980 *An Introduction to Climate*. Fifth Edition. McGraw-Hill Book Company, New York.

Trimble
2007a *Getting Started Guide GeoExplorer 2005 Series, Version 1.10*. Trimble Navigation Limited, Westminster, Colorado.

2007b *Getting Started Guide TerraSync Software, Version 3.00*. Trimble Navigation Limited, Westminster, Colorado.

2007c *Reference Manual TerraSync Software, Version 3.00*. Trimble Navigation Limited, Westminster, Colorado.

2007d *Getting Started Guide GPS Pathfinder Office Software, Version 4.00*. Trimble Navigation Limited, Westminster, Colorado.

Truman, Harry S
1949 Proclamation 2864 – Establishing the Effigy Mounds National Monument. 64th Statues at Large, 81st Congress 2d Session, 64 part 2:A371.

USDA
2006 *Land Resource Regions and Major Land Resource Areas of the United States, the Caribbean, and the Pacific Basin*. United States Department of Agriculture Handbook 296. U.S. Government Printing Office, Washington, D.C.

Ushikata
2005 *Tracon & Surveying Compasses*. Ushikata Manufacturing Company, Tokyo.

Van Nostrand, Robert G. and Kenneth L. Cook
1966 *Interpretation of Resistivity Data*. Geological Survey Professional Paper 499. United States Government Printing Office, Washington, D.C.

Von Der Osten-Woldenburg, Harald
2005 Applications of Ground-Penetrating Radar, Magnetic and Electrical Mapping, and Electromagnetic Induction Methods in Archaeological Investigations. In *Near-Surface Geophysics*, edited by Dwain K. Butler, pp. 621-626. Society of Exploration Geophysicists, Tulsa, Oklahoma.

Vobora, Robert J.
1998 *Soil Survey of Allamakee County, Iowa*. U.S. Government Printing Office, Washington, D.C.

Weymouth, John W.
1986 Geophysical Methods of Archaeological Site Surveying. In *Advances in Archaeological Method and Theory, Volume 9*, edited by Michael B. Schiffer, pp. 311-395. Academic Press, Orlando, Florida.

Witten, Alan J.
2006 *Handbook of Geophysics and Archaeology*. Equinox Publishing Ltd., London.

Zonge, Ken, Jeff Wynn, and Scott Urquhart
2005 Resistivity, Induced Polarization, and Complex Resistivity. In *Near-Surface Geophysics*, edited by Dwain K. Butler, pp. 265-300. Society of Exploration Geophysicists, Tulsa, Oklahoma.

TABLES

Table 1. Global positioning system corrected grid coordinates for the EFMO1 and EFMO2 geophysical project areas.

ID	Longitude	Latitude	HAE	Easting	Northing	MSL	Site Number	Description	Feature Type	Comment
1	-91.184923124	43.088969578	163.634	647731.979	4772293.607	195.459	13AM82	grid pt	Other	efmo1
2	-91.184821238	43.088802953	166.168	647740.672	4772275.282	197.993	13AM82	grid pt	Other	efmo1
3	-91.18471471	43.0886393	164.733	647749.737	4772257.296	196.558	13AM82	grid pt	Other	efmo1
4	-91.184621337	43.088483224	161.391	647757.712	4772240.127	193.216	13AM82	grid pt	Other	efmo1
5	-91.184402443	43.088553624	157.743	647775.359	4772248.331	189.57	13AM82	grid pt	Other	efmo1
6	-91.184183453	43.088624481	156.307	647793.013	4772256.586	188.134	13AM82	grid pt	Other	efmo1
7	-91.184279178	43.088780848	160.218	647784.846	4772273.783	192.044	13AM82	grid pt	Other	efmo1
8	-91.184380767	43.08894571	163.62	647776.181	4772291.912	195.446	13AM82	grid pt	Other	efmo1
9	-91.184190004	43.088999458	165.786	647791.578	4772298.217	197.613	13AM82	grid pt	Other	efmo1
10	-91.184255415	43.089183258	159.771	647785.812	4772318.514	191.598	13AM82	grid pt	Other	efmo1
11	-91.184504478	43.088721016	160.843	647766.652	4772266.741	192.669	13AM82	grid pt	Other	efmo1
12	-91.184601652	43.088887679	161.914	647758.342	4772285.078	193.739	13AM82	grid pt	Other	efmo1
13	-91.184703471	43.08904268	162.578	647749.682	4772302.112	194.404	13AM82	grid pt	Other	efmo1
14	-91.184416762	43.089131922	166.827	647772.803	4772312.528	198.654	13AM82	grid pt	Other	efmo1
15	-91.18024439	43.091064791	167.284	648107.747	4772534.543	199.125	13AM210	st1	Hearth	Shovel test
16	-91.180387346	43.090977655	164.287	648096.322	4772524.614	196.127	13AM210	st2		
17	-91.180501574	43.090893336	170.143	648087.228	4772515.048	201.983	13AM210	st3		

Table 1. Concluded.

ID	Longitude	Latitude	HAE	Easting	Northing	MSL	Site Number	Description	Feature Type	Comment
18	-91.18068423	43.090818087	165.457	648072.543	4772506.369	197.297	13AM210	st4		
19	-91.180839969	43.090754814	161.419	648060.019	4772499.067	193.257	13AM210	st5		
20	-91.180991549	43.09067177	165.654	648047.882	4772489.577	197.492	13AM210	st6		
21	-91.180984693	43.0907331	162.012	648048.292	4772496.4	193.851	13AM210	2	Artifact Concentration	bricks, clinker
22	-91.18119608	43.090658792	156.493	648031.266	4772487.775	188.33	13AM210	st7		
23	-91.181321205	43.090596741	152.707	648021.232	4772480.663	184.544	13AM210	st8		
24	-91.181464462	43.090483715	153.759	648009.844	4772467.858	185.596	13AM210	st9		
25	-91.183956328	43.089586722	160.663	647809.185	4772363.847	192.492	13AM82	grid pt	Other	efmo2
26	-91.18372328	43.089571518	159.604	647828.19	4772362.57	191.433	13AM82	grid pt	Other	efmo2
27	-91.183721274	43.089742395	164.359	647827.942	4772381.55	196.188	13AM82	grid pt	Other	efmo2
28	-91.18421707	43.089574437	161.464	647787.992	4772362.023	193.292	13AM82	grid pt	Other	efmo2
29	-91.184226669	43.089740175	169.611	647786.813	4772380.412	201.439	13AM82	grid pt	Other	efmo2

Table 2. Acquisition and instrumentation information for the single fluxgate gradiometer survey used in the grid input template at the EFMO1 geophysical project area (Site 13AM82).

GENERAL			
Acquisition	Value	Instrumentation	Value
Sitename	EFMO1	Survey Type	Gradiometer
Map Reference	Prairie Du Chien, Iowa-Wisconsin 7.5 minute quadrangle	Instrument	FM256
Dir. 1st Traverse	Grid N	Units	nT
Grid Length (x)	20 m	Range	AUTO
Sample Interval (x)	0.125 m	Log Zero Drift	Off
Grid Width (y)	20 m	Baud Rate	19200
Traverse Interval (y)	1.0 m	Data Format	HEX D+R
Traverse Mode	ZigZag	Computer Buffer Size	32767
FILE NOMINCLATURE	Raw Data	Processed Data	Corrected Data
Processing Software	GEOPLOT		
Grid	sg1-sg8		
Mesh	sgm		
Composite	sgc	sgcz,sgczi,sgczil, sgczilr	

Table 3. Acquisition and instrumentation information for the single fluxgate gradiometer survey used in the grid input template at the EFMO2 geophysical project area (Site 13AM82).

GENERAL			
Acquisition	Value	Instrumentation	Value
Sitename	EFMO2	Survey Type	Gradiometer
Map Reference	Prairie Du Chien, Iowa-Wisconsin 7.5 minute quadrangle	Instrument	FM256
Dir. 1st Traverse	Magnetic N	Units	nT
Grid Length (x)	20 m	Range	AUTO
Sample Interval (x)	0.125 m	Log Zero Drift	Off
Grid Width (y)	20 m	Baud Rate	19200
Traverse Interval (y)	1.0 m	Data Format	HEX D+R
Traverse Mode	ZigZag	Computer Buffer Size	32767
FILE NOMINCLATURE	Raw Data	Processed Data	Corrected Data
Processing Software	GEOPLOT		
Grid	g1-g2		
Mesh	gm		
Composite	gc	gcz,gczi,gczil,gczilr	

Table 4. Acquisition and instrumentation information for the dual fluxgate gradiometer survey used in the grid input template at the EFMO1 geophysical project area (Site 13AM82).

GENERAL			
Acquisition	Value	Instrumentation	Value
Sitename	EFMO1	Survey Type	Dual Gradiometer
Map Reference	Prairie Du Chien, Iowa-Wisconsin 7.5 minute quadrangle	Instrument	Bartington Grad601-2
Dir. 1st Traverse	Grid N	Units	nT
Grid Length (x)	20 m	Range	AUTO
Sample Interval (x)	0.125 m	Log Zero Drift	Off
Grid Width (y)	20 m	Baud Rate	19200
Traverse Interval (y)	1.0 m	Number of Sensors (tubes)	2
Traverse Mode	ZigZag	Download Software	Bartington GRAD601
FILE NOMINCLATURE	Raw Data	Processed Data	Corrected Data
Processing Software	Archeosurveyor		
Grid	dg01-dg08		
Composite	dgc	dgccz, dgcczi,dgczil	

Table 5. Acquisition and instrumentation information for the ground conductivity survey used in the grid input template at the EFMO1 geophysical project area (Site 13AM82).

Acquisition	Value	Instrumentation	Value
Sitename	EFMO1	Survey Type	EM
Map Reference	Prairie Du Chien, Iowa-Wisconsin 7.5 minute quadrangle	Instrument	EM38
Dir. 1st Traverse	Grid N	Units	mS/m
Grid Length (x)	20 m		
Sample Interval (x)	0.25 m		
Grid Width (y)	20 m		
Traverse Interval (y)	1.0 m		
Traverse Mode	Parallel		
FILE NOMINCLATURE	Raw Data	Processed Data	Corrected Data
Processing Software	GEOPLOT		
Grid	q1-q8		
Mesh	qm		
Composite	qc	qce,qcei,qceih, qceihr	

Table 6. Acquisition and instrumentation information for the ground conductivity survey used in the grid input template at the EFMO2 geophysical project area (Site 13AM82).

Acquisition	Value	Instrumentation	Value
Sitename	EFMO2	Survey Type	EM
Map Reference	Prairie Du Chien, Iowa-Wisconsin 7.5 minute quadrangle	Instrument	EM38
Dir. 1st Traverse	Magnetic N	Units	mS/m
Grid Length (x)	20 m		
Sample Interval (x)	0.25 m		
Grid Width (y)	20 m		
Traverse Interval (y)	1.0 m		
Traverse Mode	Parallel		
FILE NOMINCLATURE	Raw Data	Processed Data	Corrected Data
Processing Software	GEOPLOT		
Grid	q1-q2		
Mesh	qm		
Composite	qc	qci,qcih,qcihr	

Table 7. Acquisition and instrumentation information for the resistance survey used in the grid input template at the EFMO1 geophysical project area (Site 13AM82).

GENERAL			
Acquisition	Value	Instrumentation	value
Sitename	EFMO1	Survey Type	Resistance
Map Reference	Prairie Du Chien, Iowa-Wisconsin 7.5 minute quadrangle	Instrument	RM15
Dir. 1st Traverse	Grid N	Units	Ohm
Grid Length (x)	20 m	Current Range	AUTO
Sample Interval (x)	0.5 m	Gain Range	AUTO
Grid Width (y)	20 m	Baud Rate	9600
Traverse Interval (y)	1.0 m	Frequency	137 Hz
Traverse Mode	Zigzag	High Pass Filter	13 Hz
ACCESSORIES			
	Accessories	value	
	Array Hardware	PA5	
	Interface	AD1	
	Log Mode	Single	
	Configuration	Twin	
	Probe Spacing	0.5	
FILE NOMINCLATURE	Raw Data	Processed Data	Corrected Data
Processing Software	GEOPLOT		
Grid	r1-r8		
Mesh	rm		
Composite	rc	rcd,rcdi,rcdih,rcdihr	

Table 8. Acquisition and instrumentation information for the resistance survey used in the grid input template at the EFMO2 geophysical project area (Site 13AM82).

GENERAL			
Acquisition	Value	Instrumentation	value
Sitename	EFMO2	Survey Type	Resistance
Map Reference	Prairie Du Chien, Iowa-Wisconsin 7.5 minute quadrangle	Instrument	RM15
Dir. 1st Traverse	N	Units	Ohm
Grid Length (x)	20 m	Current Range	AUTO
Sample Interval (x)	0.5 m	Gain Range	AUTO
Grid Width (y)	20 m	Baud Rate	9600
Traverse Interval (y)	1.0 m	Frequency	137 Hz
Traverse Mode	Zigzag	High Pass Filter	13 Hz
ACCESSORIES			
	Accessories	Value	
	Array Hardware	PA5	
	Interface	AD1	
	Log Mode	Single	
	Configuration	Twin	
	Probe Spacing	0.5	
FILE NOMINCLATURE	Raw Data	Processed Data	Corrected Data
Processing Software	GEOPLOT		
Grid	r1-r2		
Mesh	rm		
Composite	rc	rcd,rcdi,rcdih,rcdihr	

Table 9. Acquisition and instrumentation information for the ground-penetrating radar survey at the EFMO1 geophysical project area (Site 13AM82).

GENERAL			
Acquisition	Value	Instrumentation	Value
File Nam	EFMOA	Survey Type	GPR
Number of Profile Lines	121	Instrument	GSSI TerraSIRch SIR 3000
Dir. 1st Traverse	Grid N	Samples/scan	512
Grid Length (x)	20 m	Bits/sample	16
Scans/meter	50	Scans/second	50
Grid Width (y)	20 m	Meters/mark	1
Traverse Interval (y)	0.5 m	Diel Constant	8
Traverse Mode	Zigzag	Antenna	400 mHz
ACCESSORIES			
	Channel(s)	1	
	Range Gain (dB)	-20.0 34.0 34.0 45.0 49.0	
	Position Correction	0 ns	
	Vertical IIR LP N = 1F	800 mHz	
	Vertical IIR HP N = 1F	100 mHz	
	Position (ns)	0	
	Range (ns)	100	

FIGURES

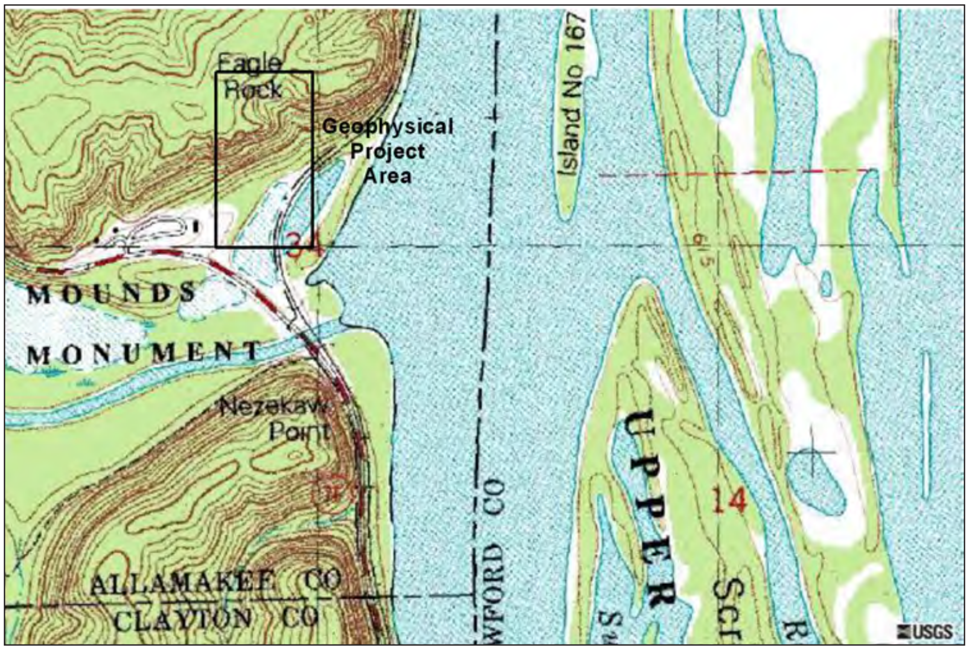

a) topographic map of the Effigy Mounds National Monument 6 km NE of Prairie du Chien, Wisconson (USGS topo map dated 01 Jul 1983)

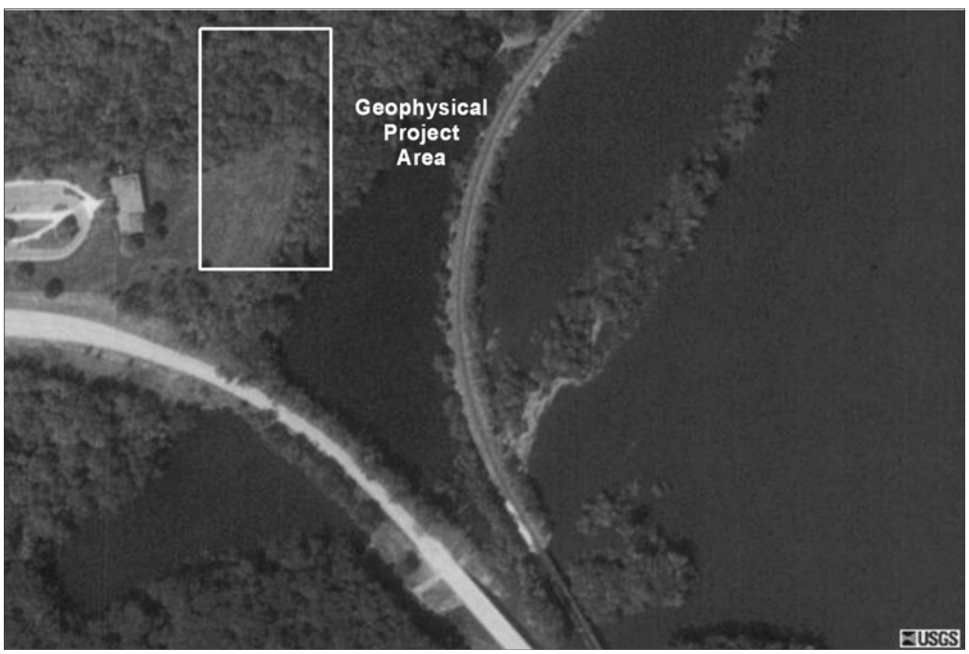

b) aerial photograph of the Effigy Mounds National Monument 6 km NE of Prairie du Chien, Wisconson (USGS aerial photo dated 17 May 1983)

Figure 1. Location of the geophysical project area on the Nezekaw Terrace at Effigy Mounds National Monument in Allamakee County, Iowa.

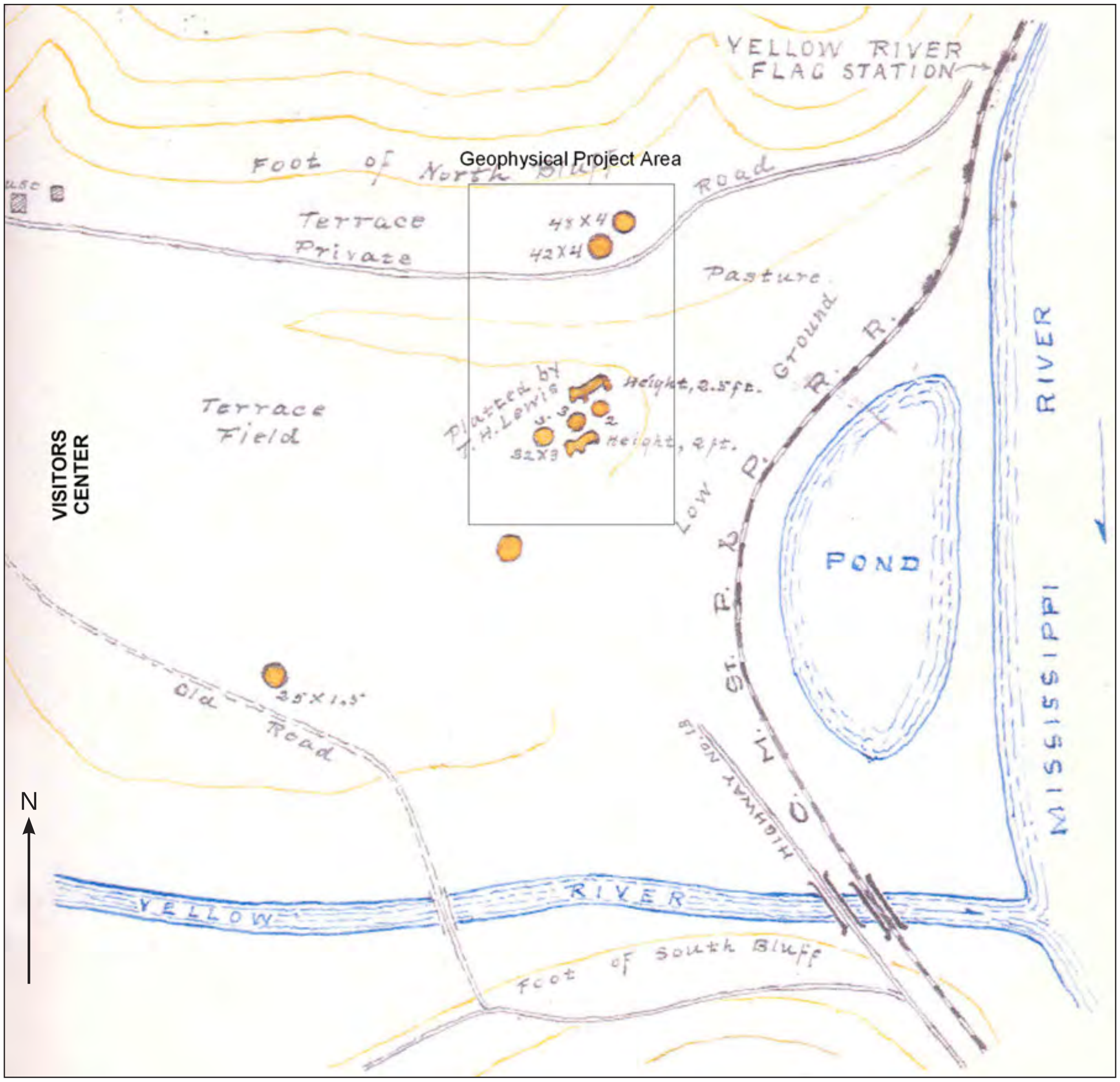

Figure 2. Orr's map of Lewis's notes on the mounds located on the Nezekaw Terrace with the location of the geophysical project area (adapted from Orr 1939:107).

Figure 3. General view of the EFMO1 project area from the northeastern corner (view to the southwest).

Figure 4. General view of the EFMO2 project area from the southeast corner of the geophysical grid (view to the west northwest).

EFFIGY MOUNDS

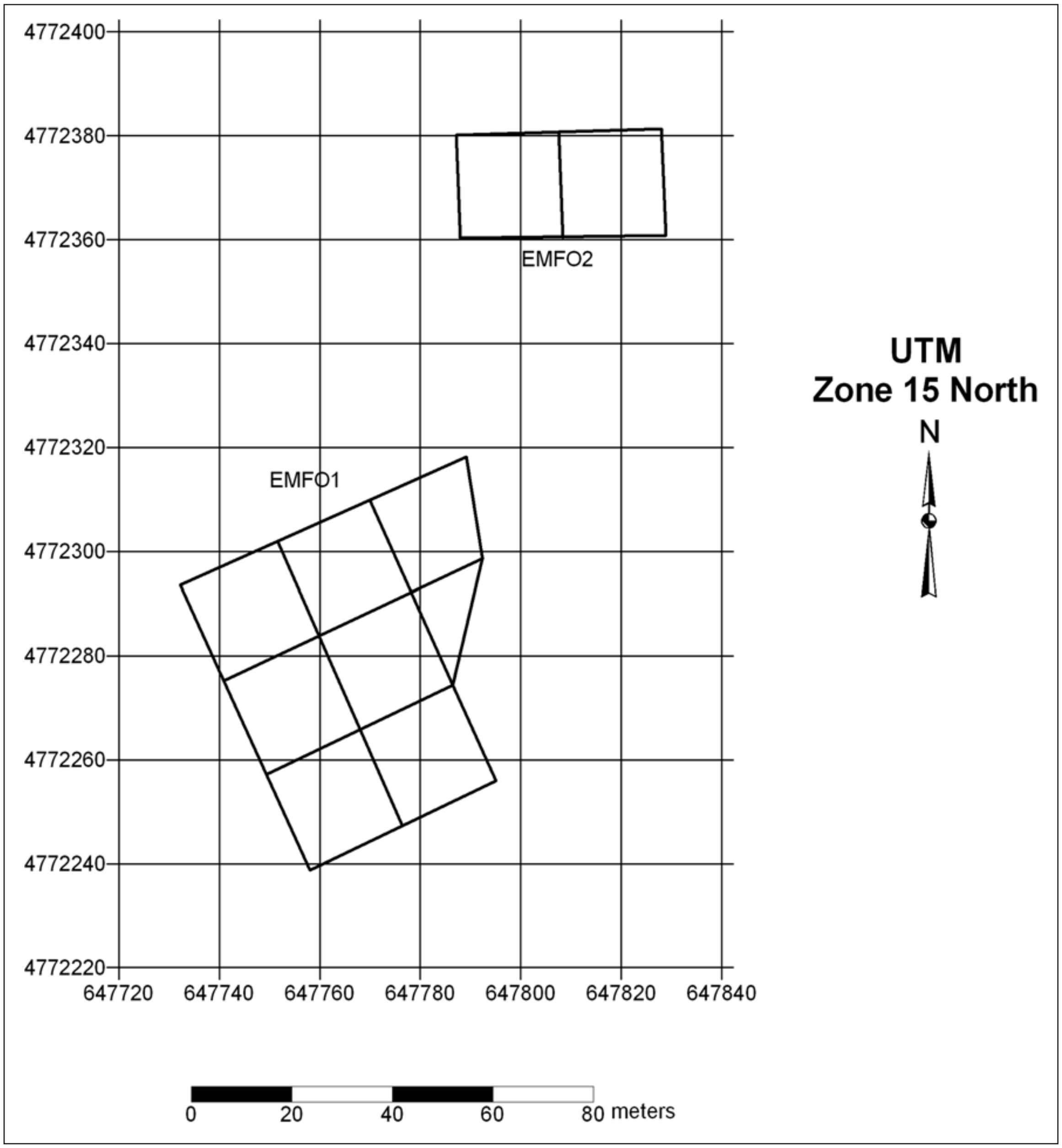

Figure 5. Location of the two geophysical survey grid locations at Effigy Mounds National Monument.

Figure 6. Laying out the survey ropes at the EFMO1 geophysical project area (view to the notheast).

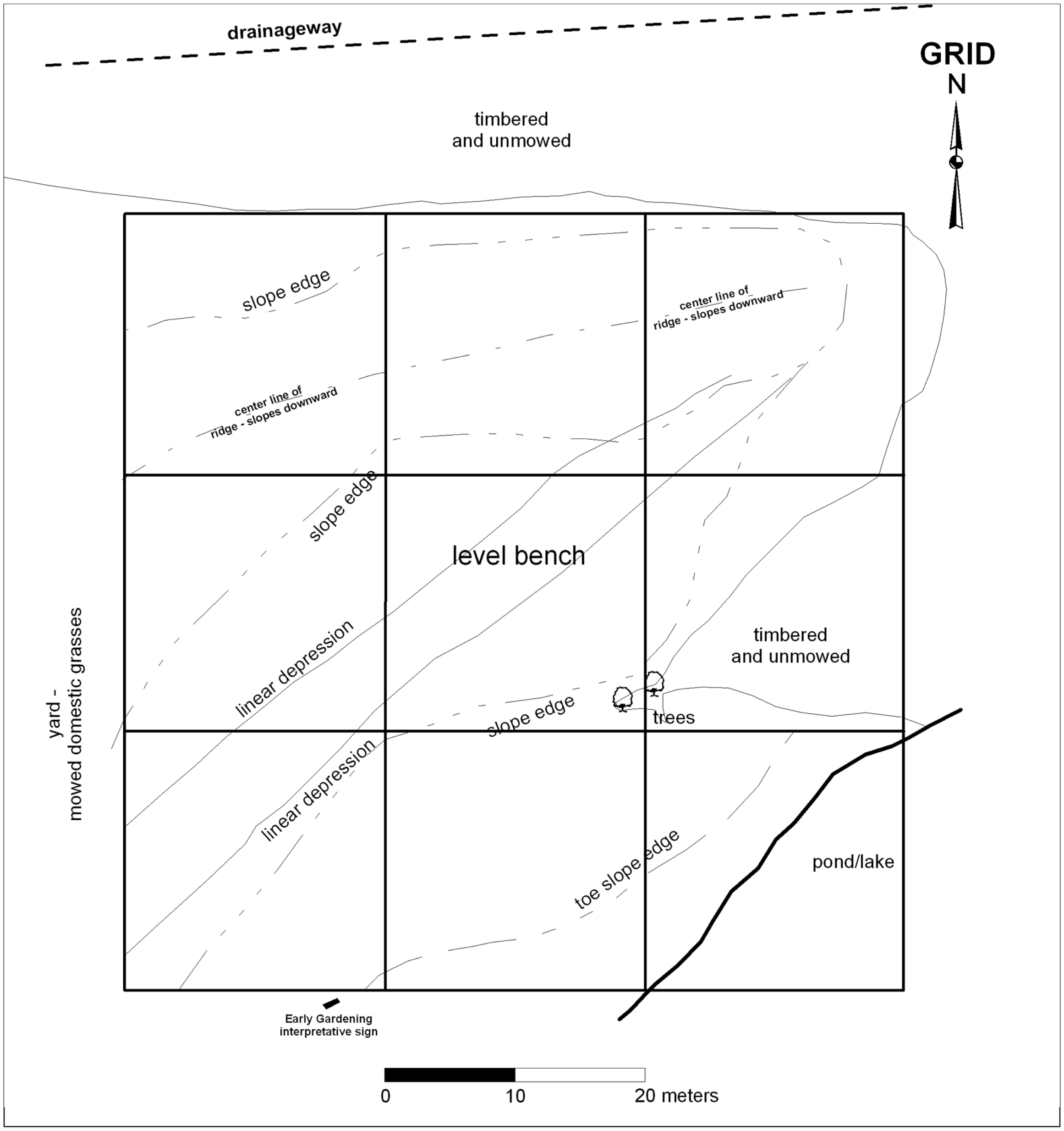

Figure 7. Sketch map of the EFMO1 geophysical project area.

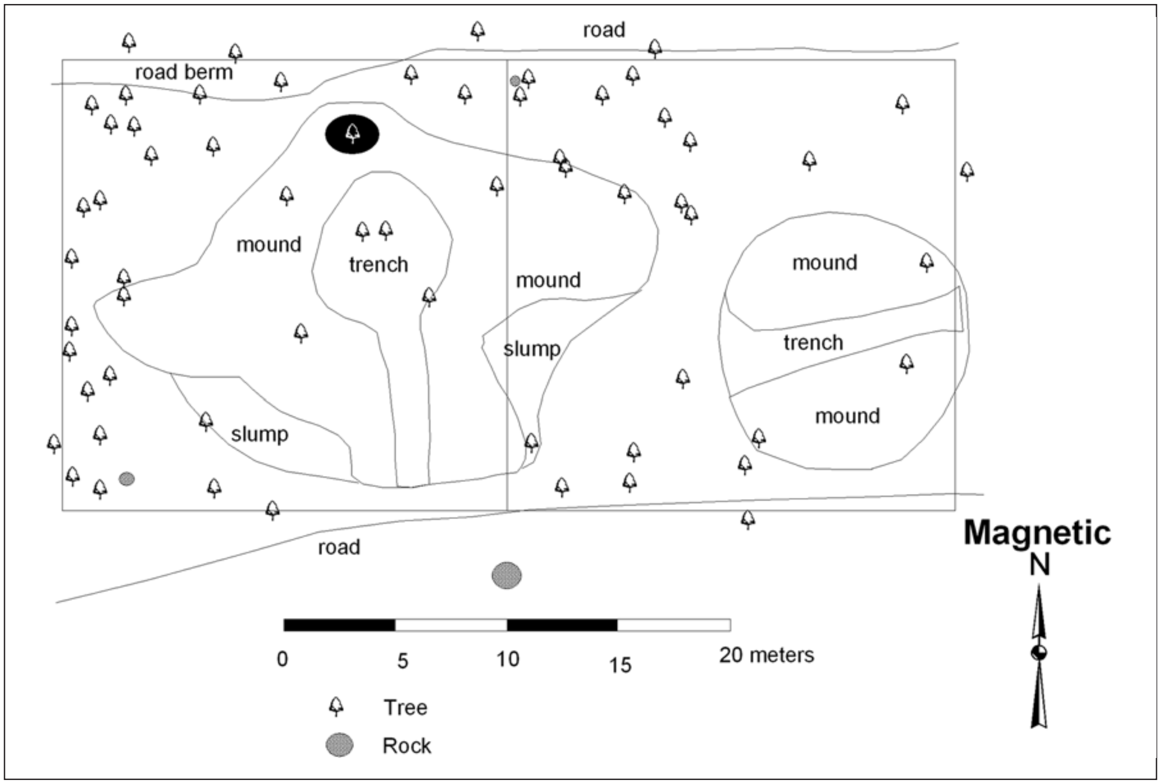

Figure 8. Sketch map of the EFMO2 geophysical project area.

Figure 9. Conducting the magnetic survey at EFMO2 with the single fluxgate gradiometer (view to the northwest).

Figure 10. Conducting the magnetic survey at EFMO1 with a dual fluxgate gradiometer (view to the south).

Figure 11. Conducting the conductivity survey with a ground conductivity meter at EMFO2 (view to the west).

Figure 12. Conducting the resistance survey with a resistance meter and twin probe array at EFMO1 (view to the north northwest).

Figure 13. Conducting the ground penetrating radar survey with a gpr cart and 400 mHz antenna (view to the west northwest).

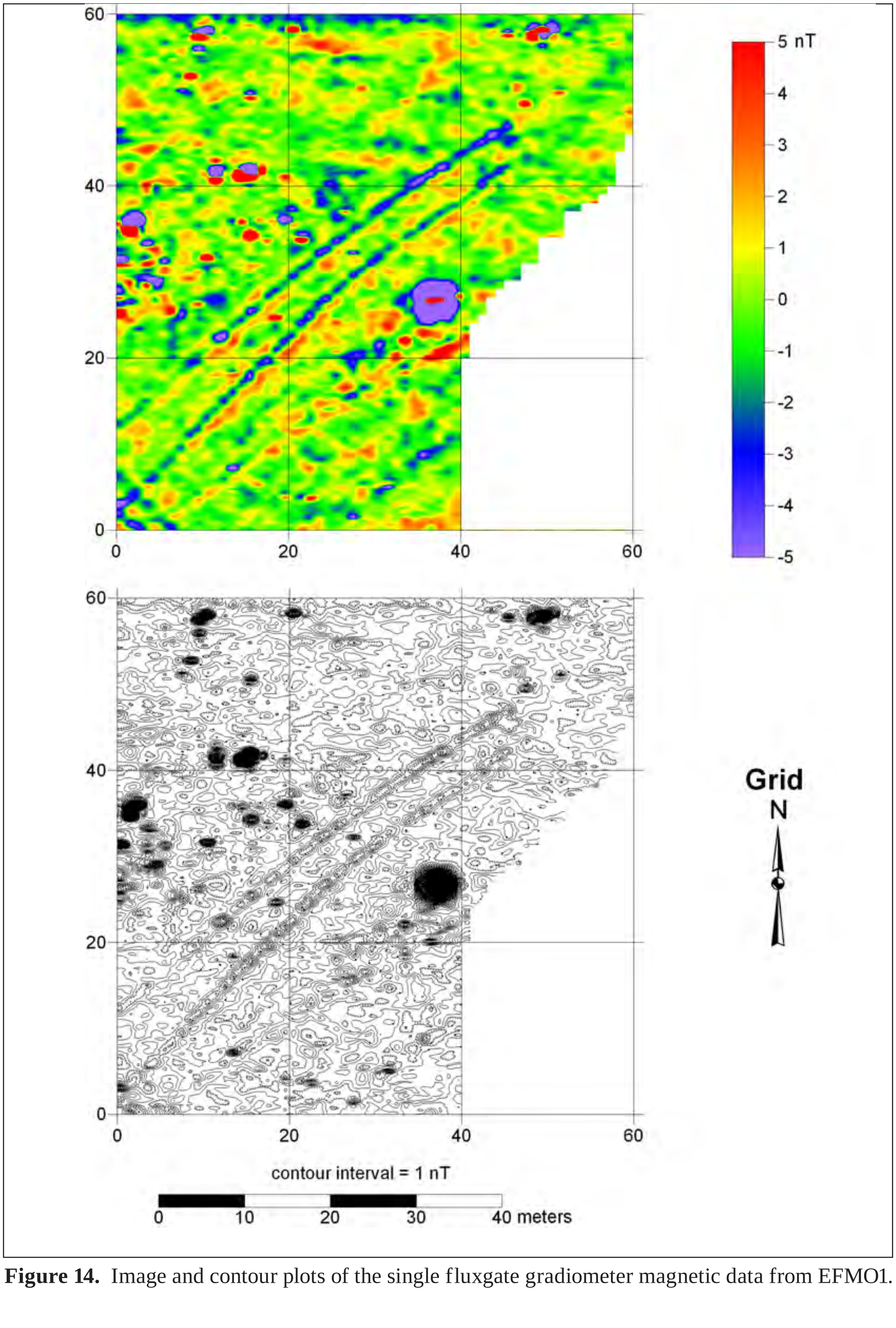

Figure 14. Image and contour plots of the single fluxgate gradiometer magnetic data from EFMO1.

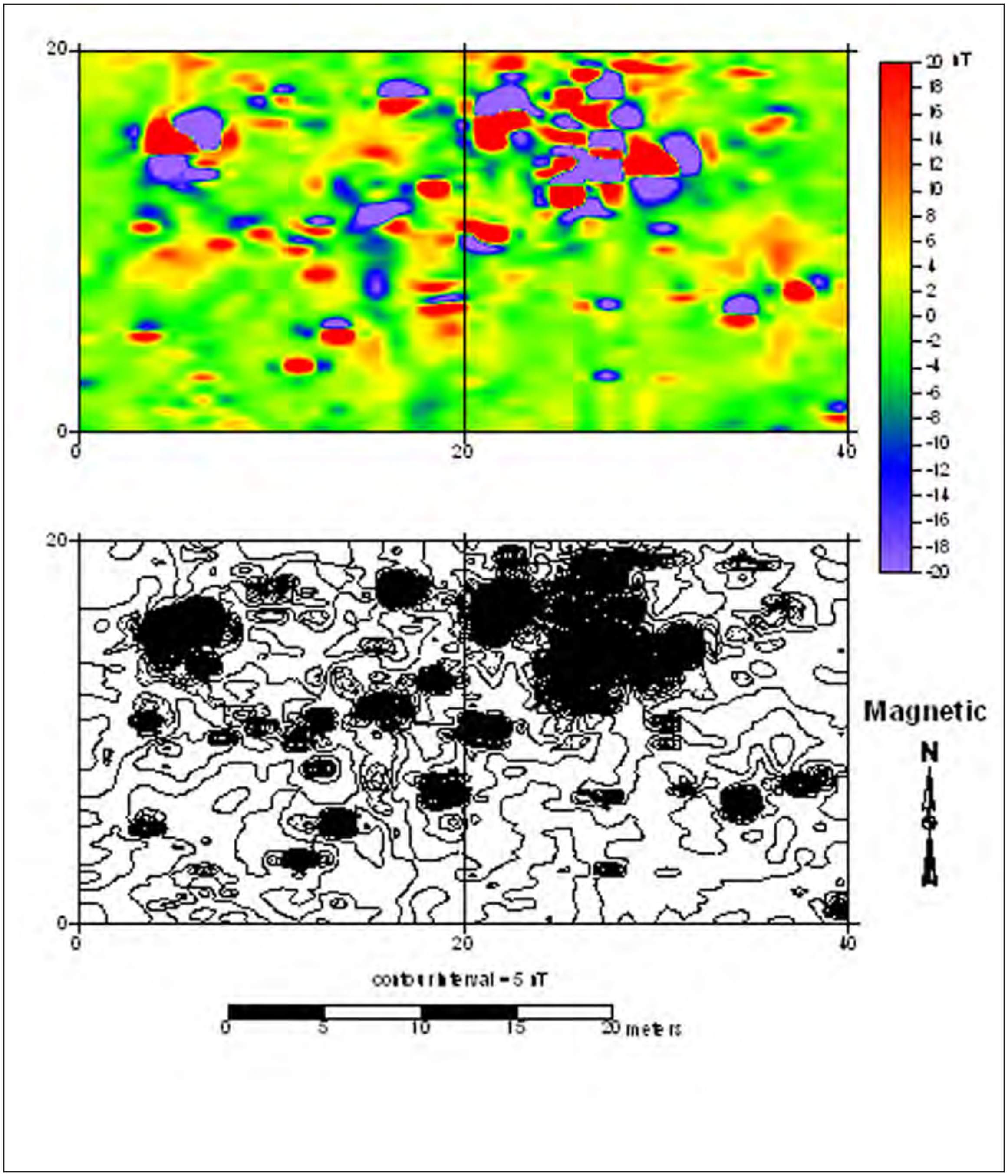

Figure 15. Image and contour plots of the single fluxgate gradiometer magnetic data from EFMO2.

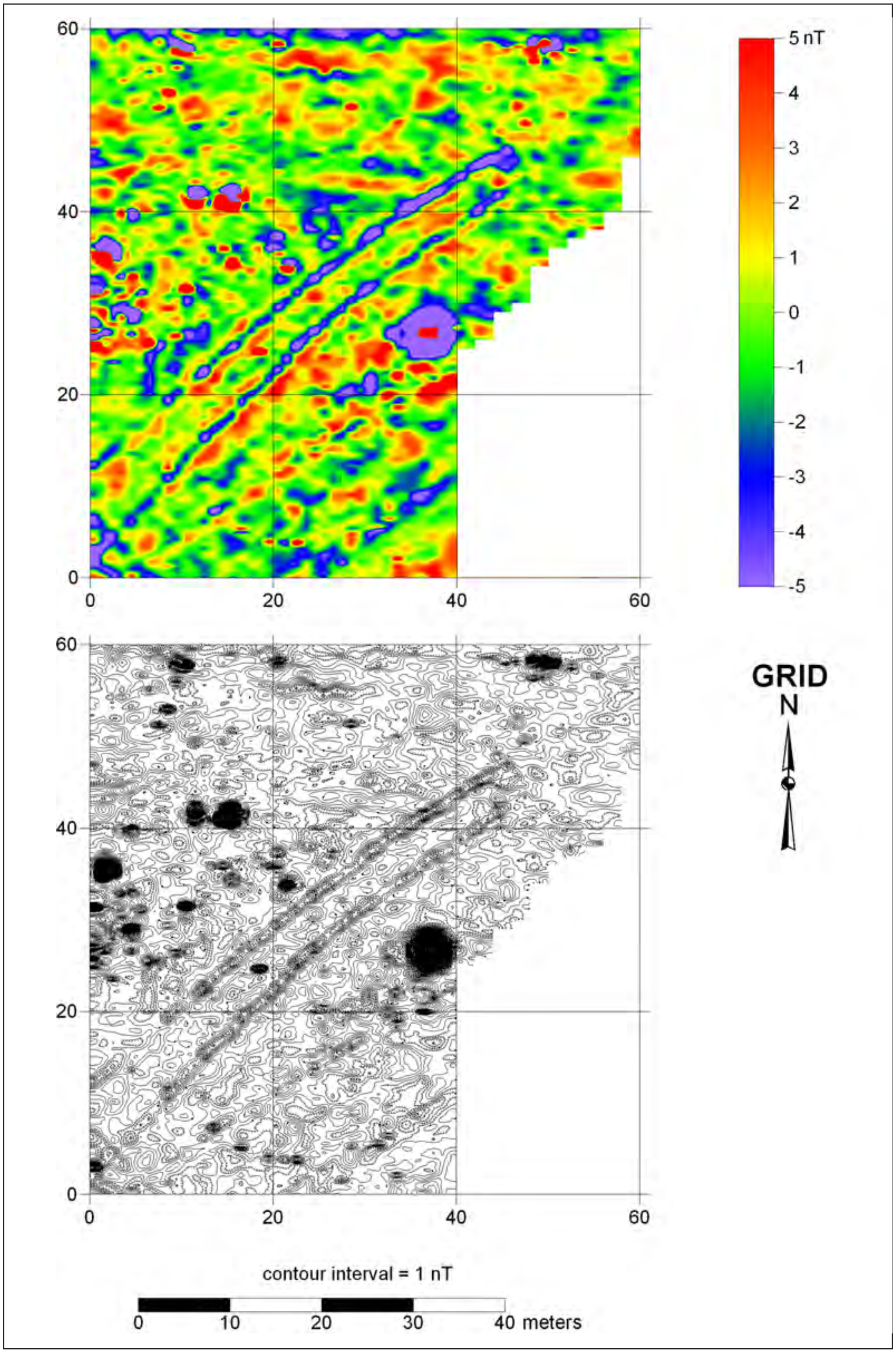

Figure 16. Image and contour plots of the dual fluxgate gradiometer magnetic data from EFMO1.

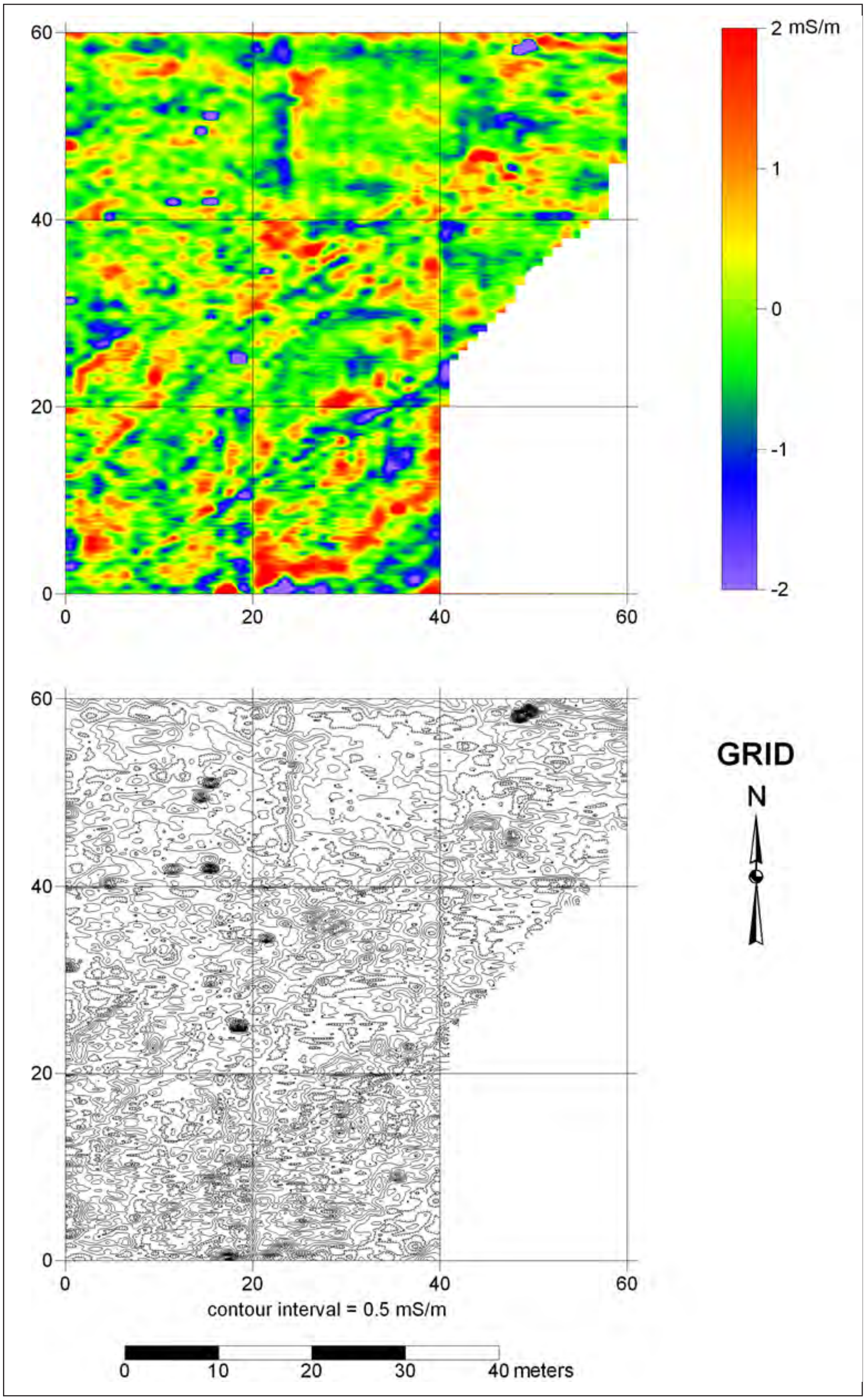

Figure 17. Image and contour plots of the conductivity data from EFMO1.

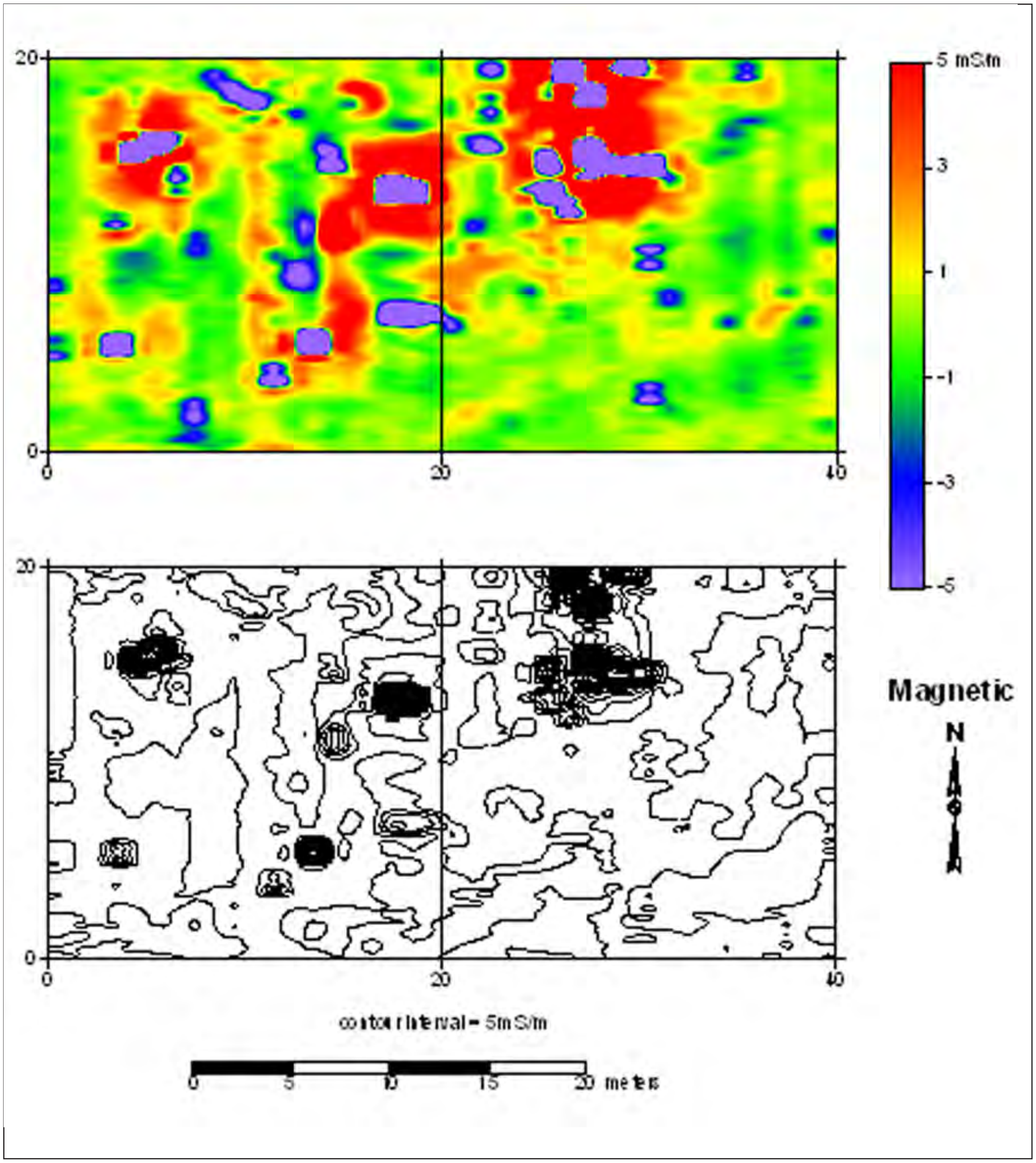

Figure 18. Image and contour plots of the conductivity data from EFMO2.

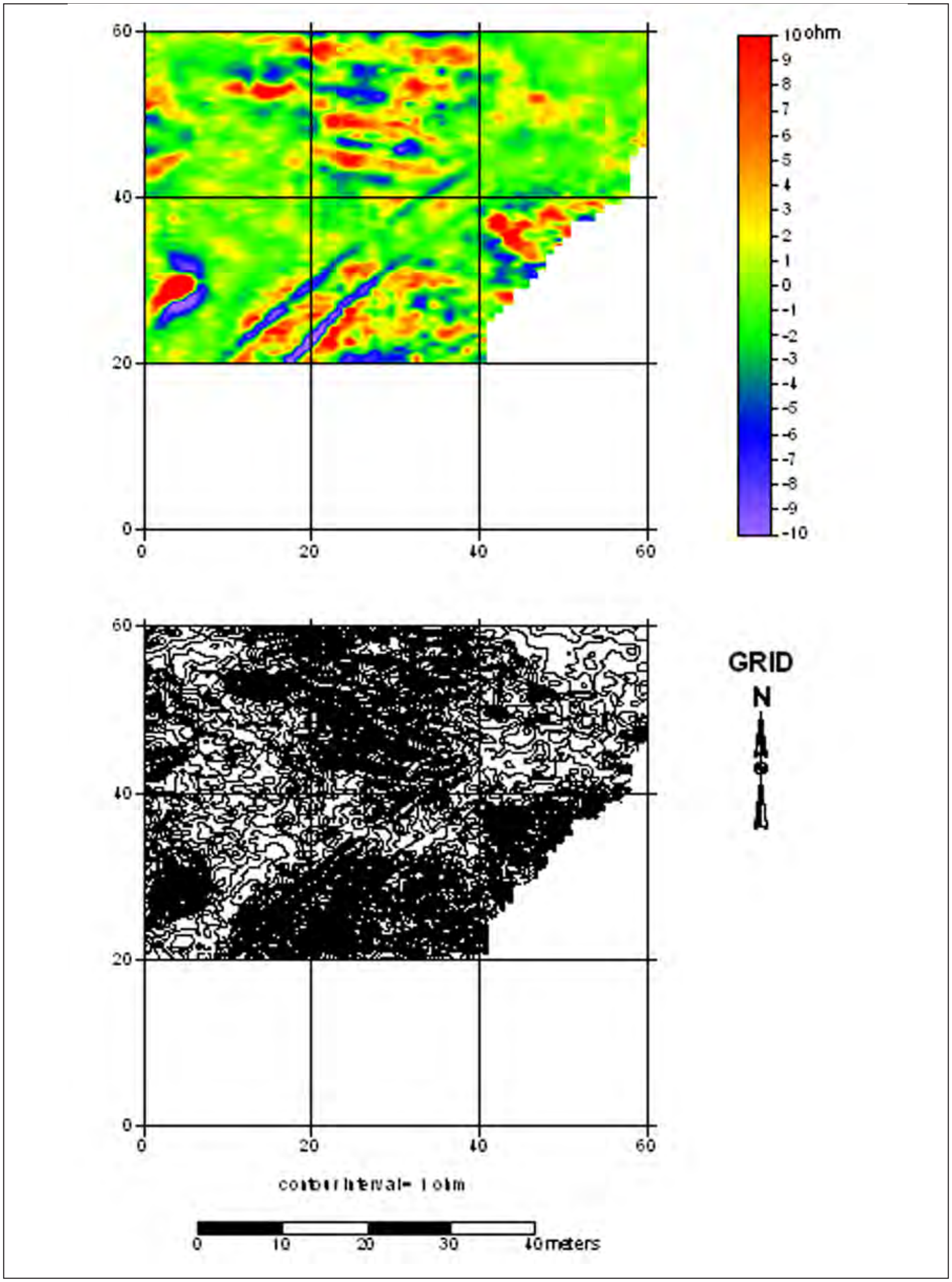

Figure 19. Image and contour plots of the resistance data from EFMO1.

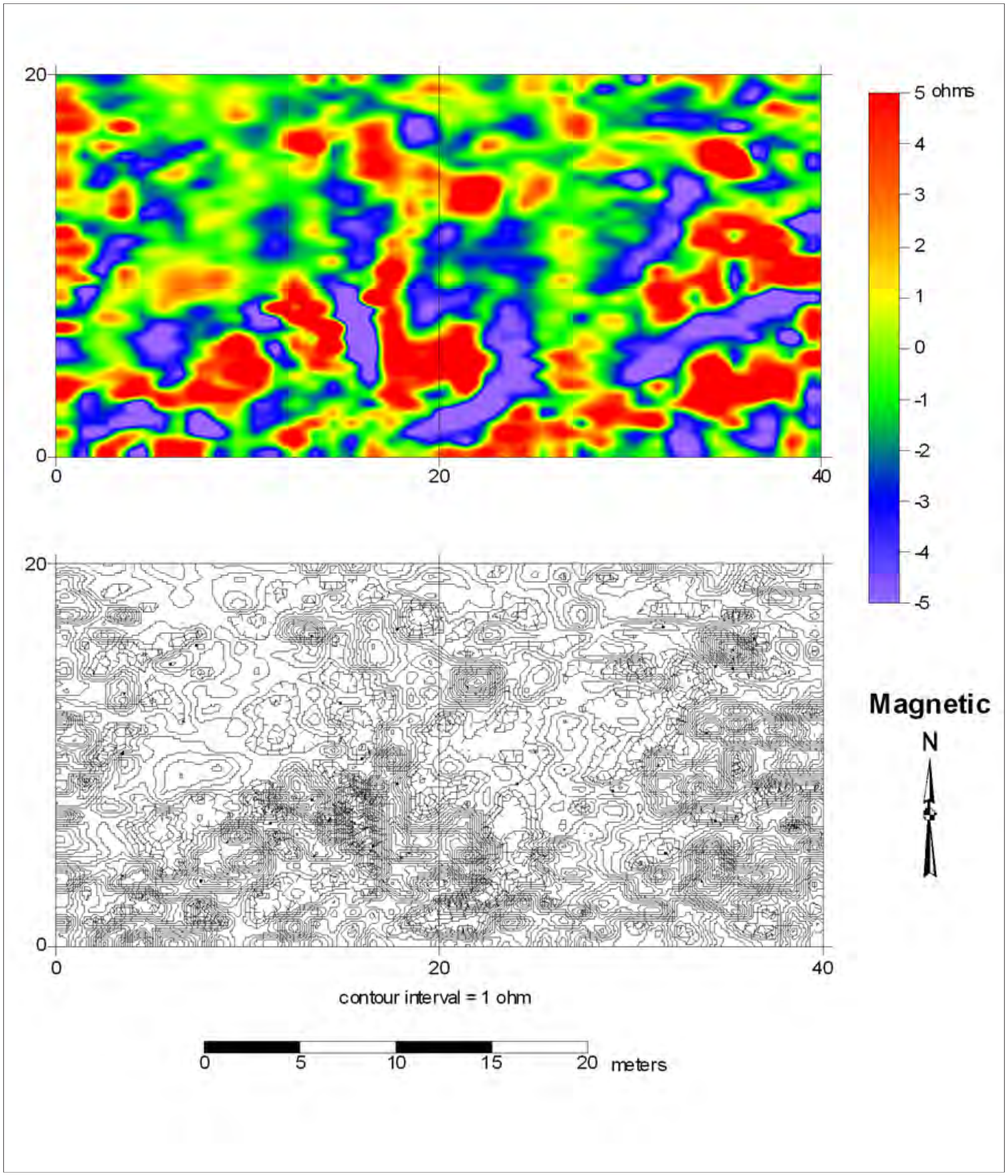

Figure 20. Image and contour plots of the resistance data from EFMO2.

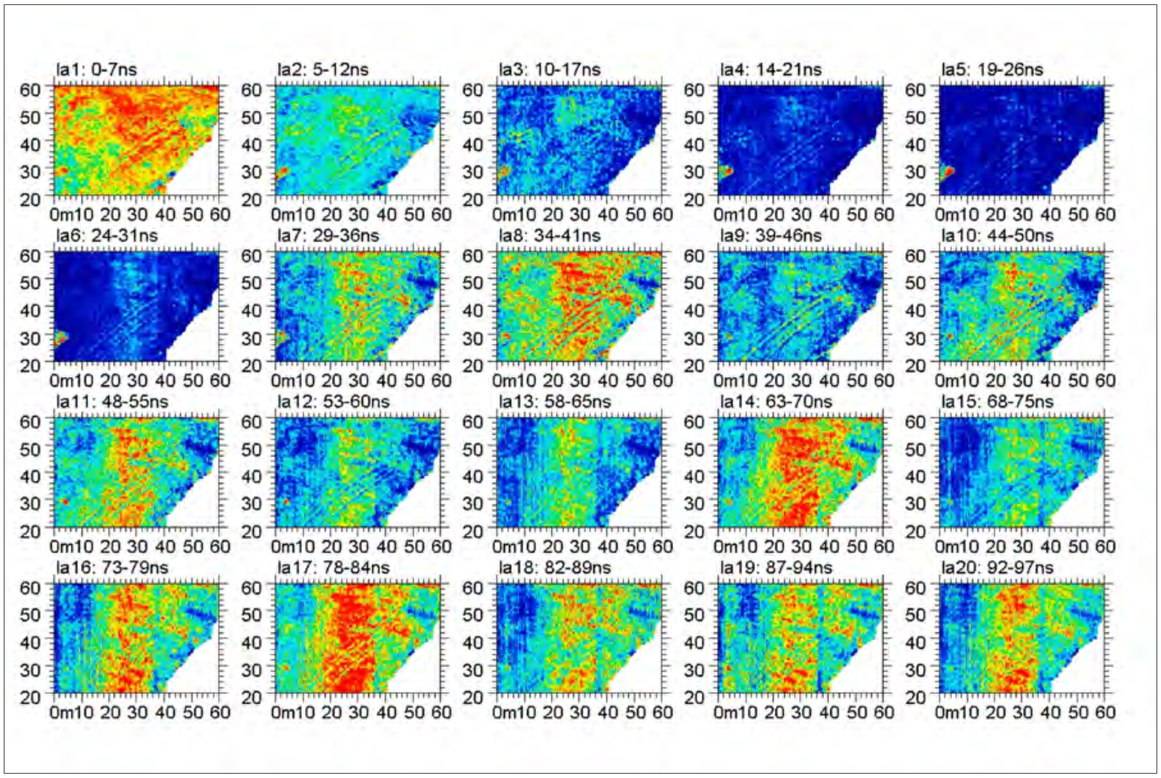

Figure 21. Time slice gpr data from the EFMO1 geophysical area.

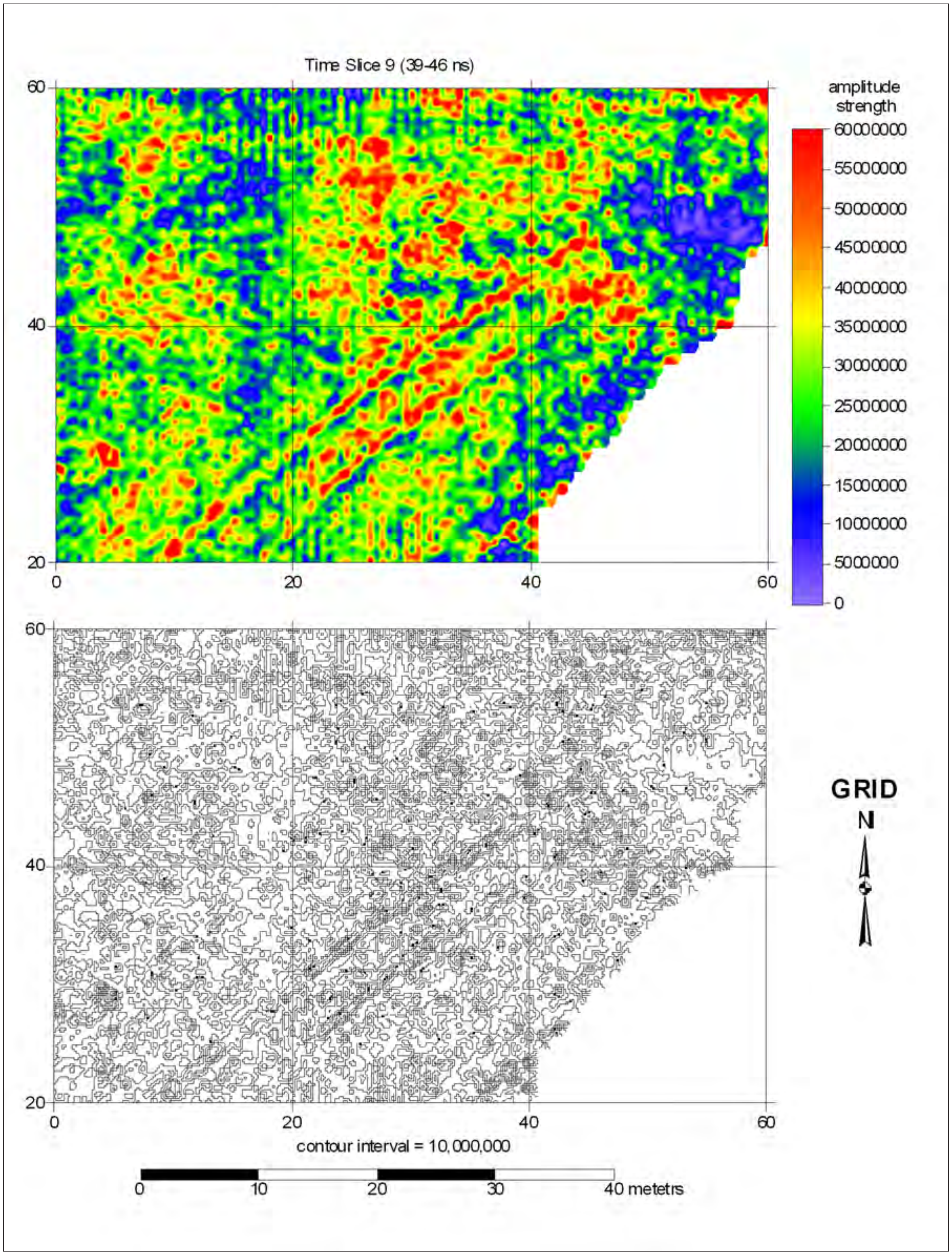

Figure 22. Image and contour plots of the time slice 9 ground penetrating radar data from the northern portion of EFMO1.

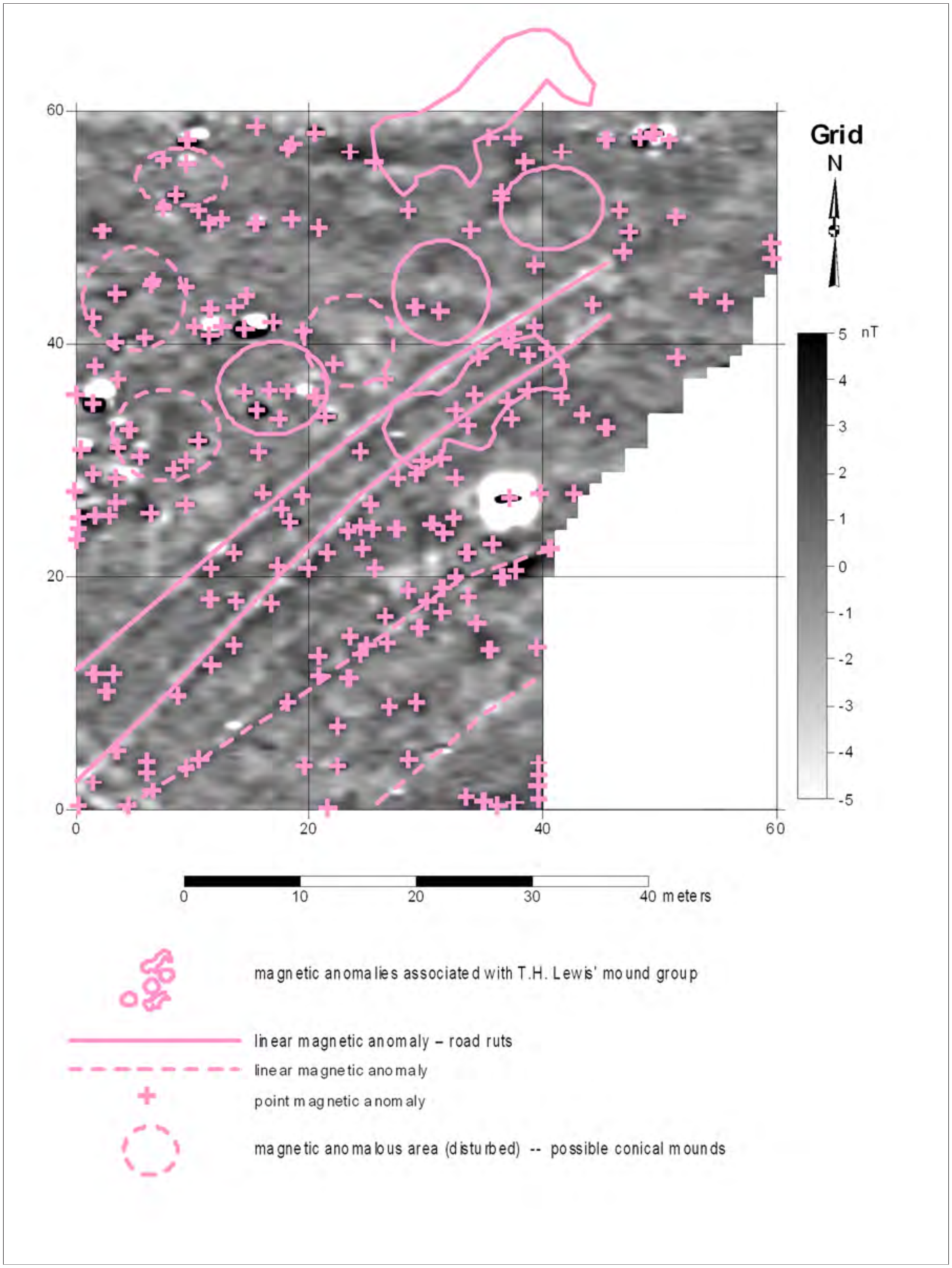

Figure 23. Interpretation of the magnetic data from the single fluxgate gradiometer in the EFMO1 geophysical project area.

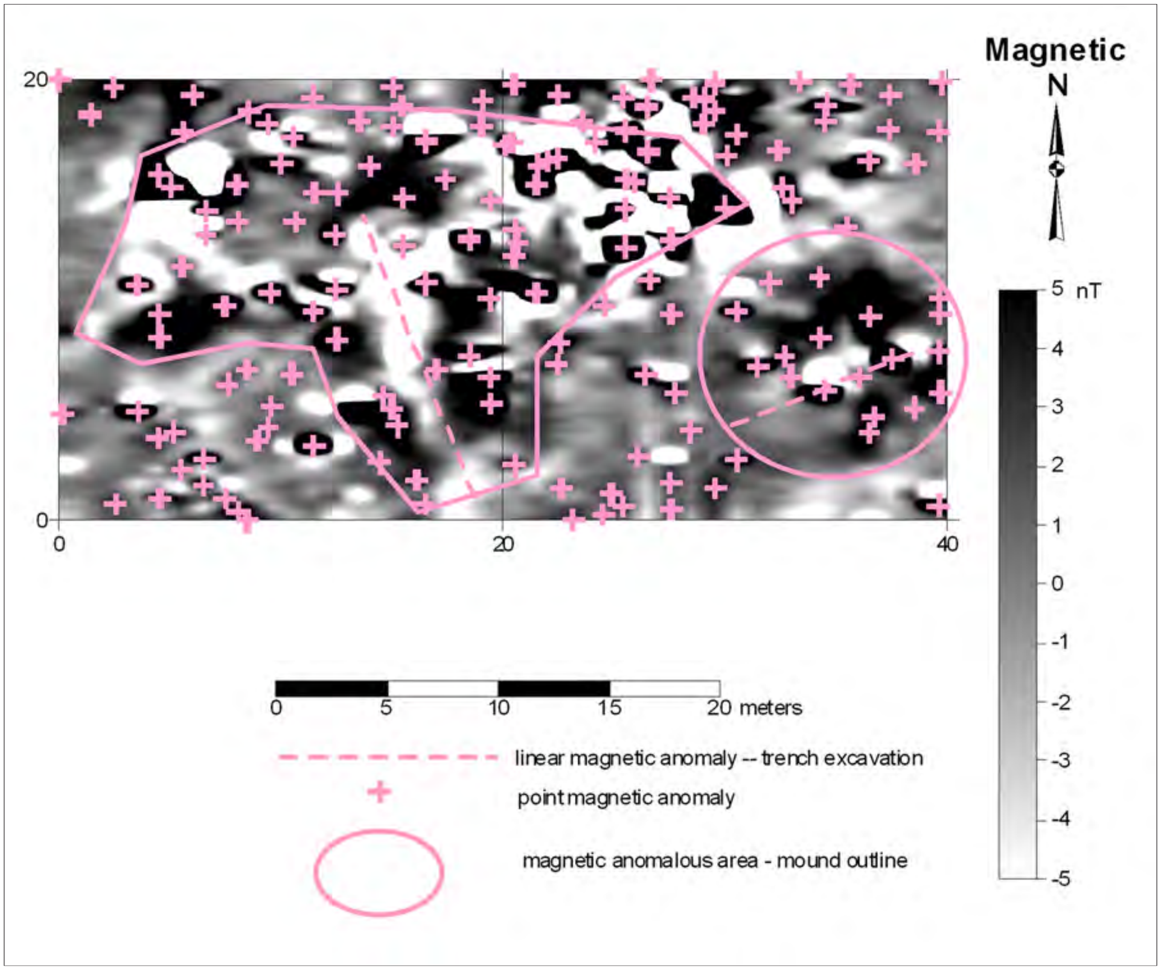

Figure 24. Interpretation of the magnetic data from the single fluxgate gradiometer in the EFMO2 geophysical project area.

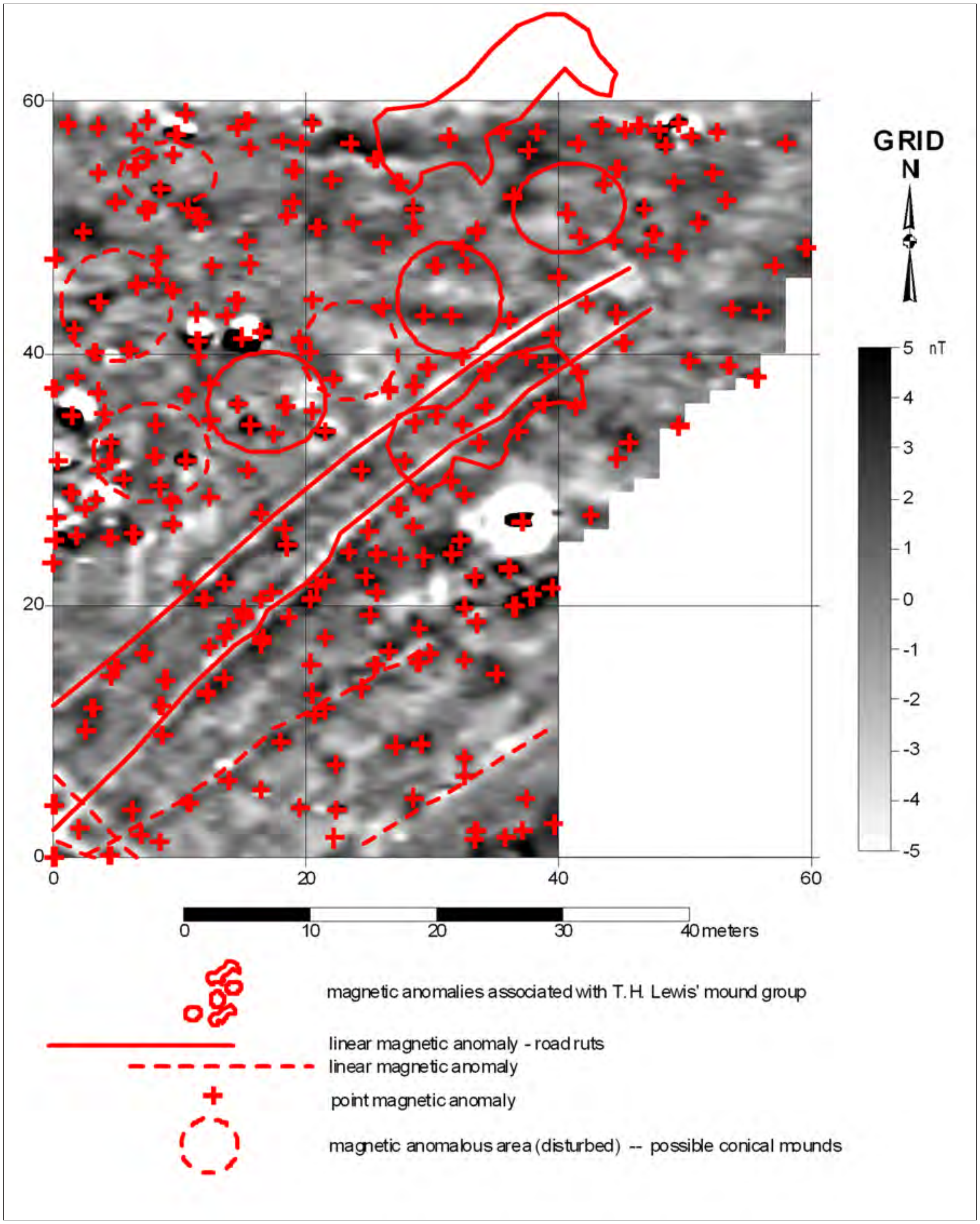

Figure 25. Interpretation of the magnetic data from the dual fluxgate gradiometer in the EFMO1 geophysical project area.

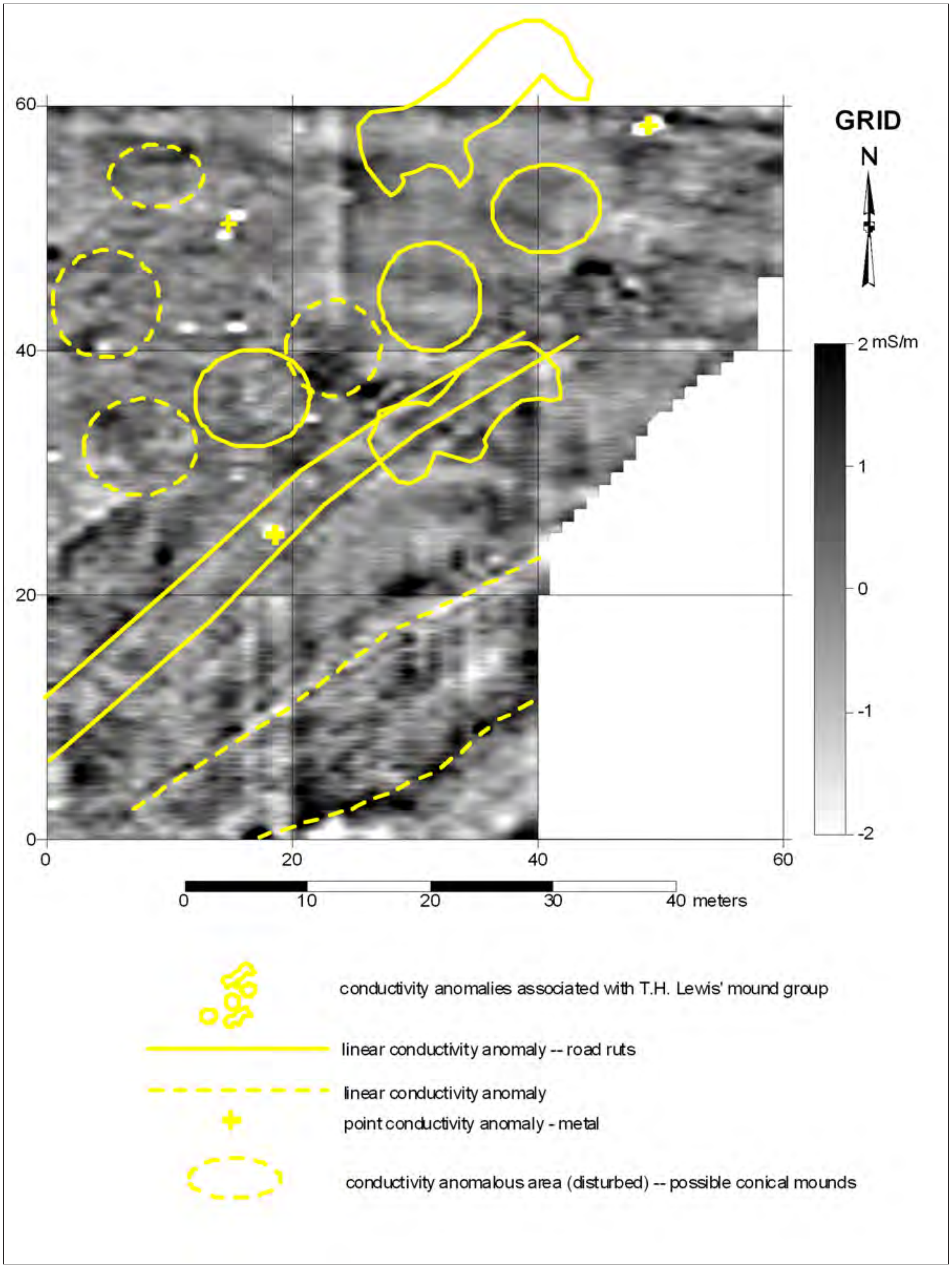

Figure 26. Interpretation of the conductivity data from the EFMO1 geophysical project area.

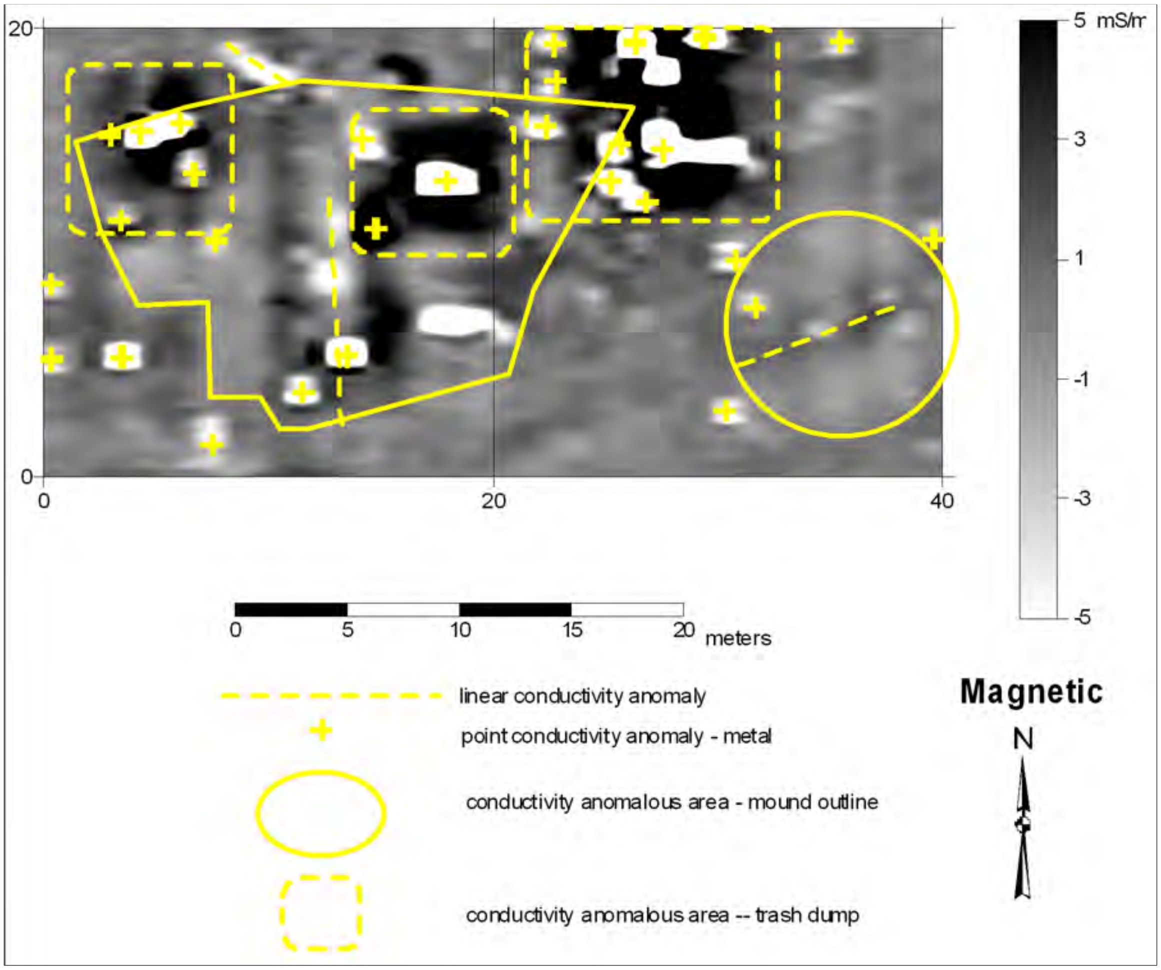

Figure 27. Interpretation of the conductivity data from the EFMO2 geophysical project area.

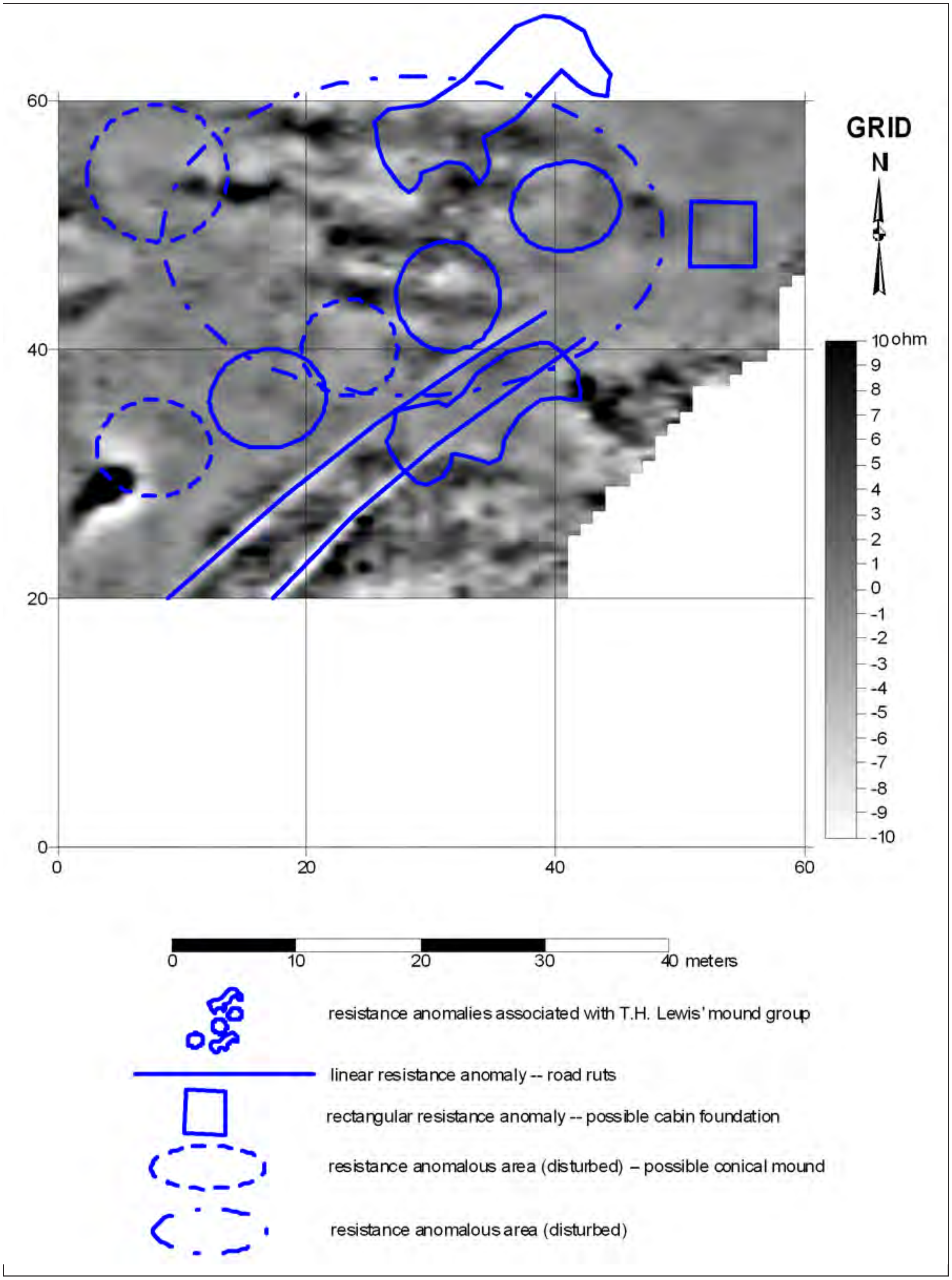

Figure 28. Interpretation of the resistance data from the EFMO1 geophysical project area.

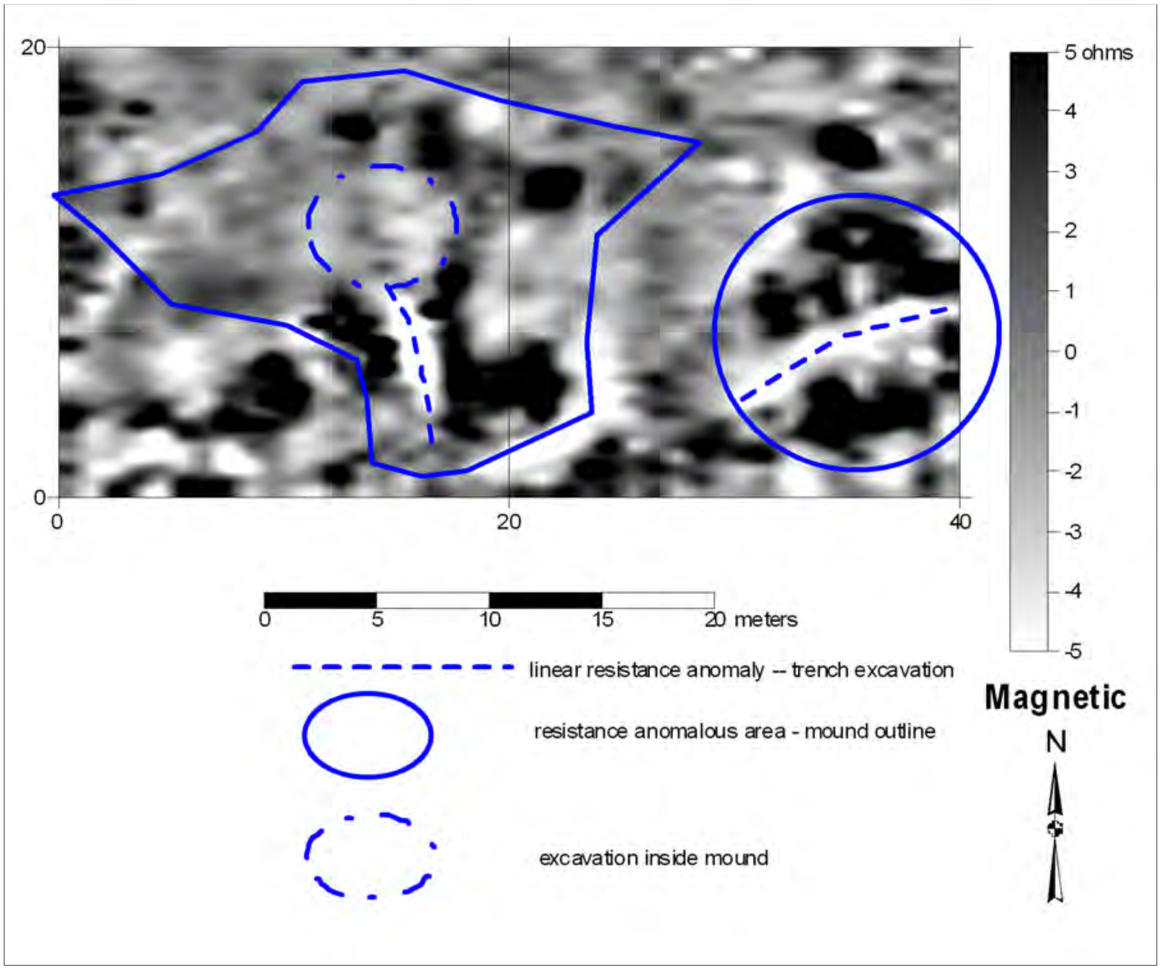

Figure 29. Interpretation of the resistance data from the EFMO2 geophysical project area.

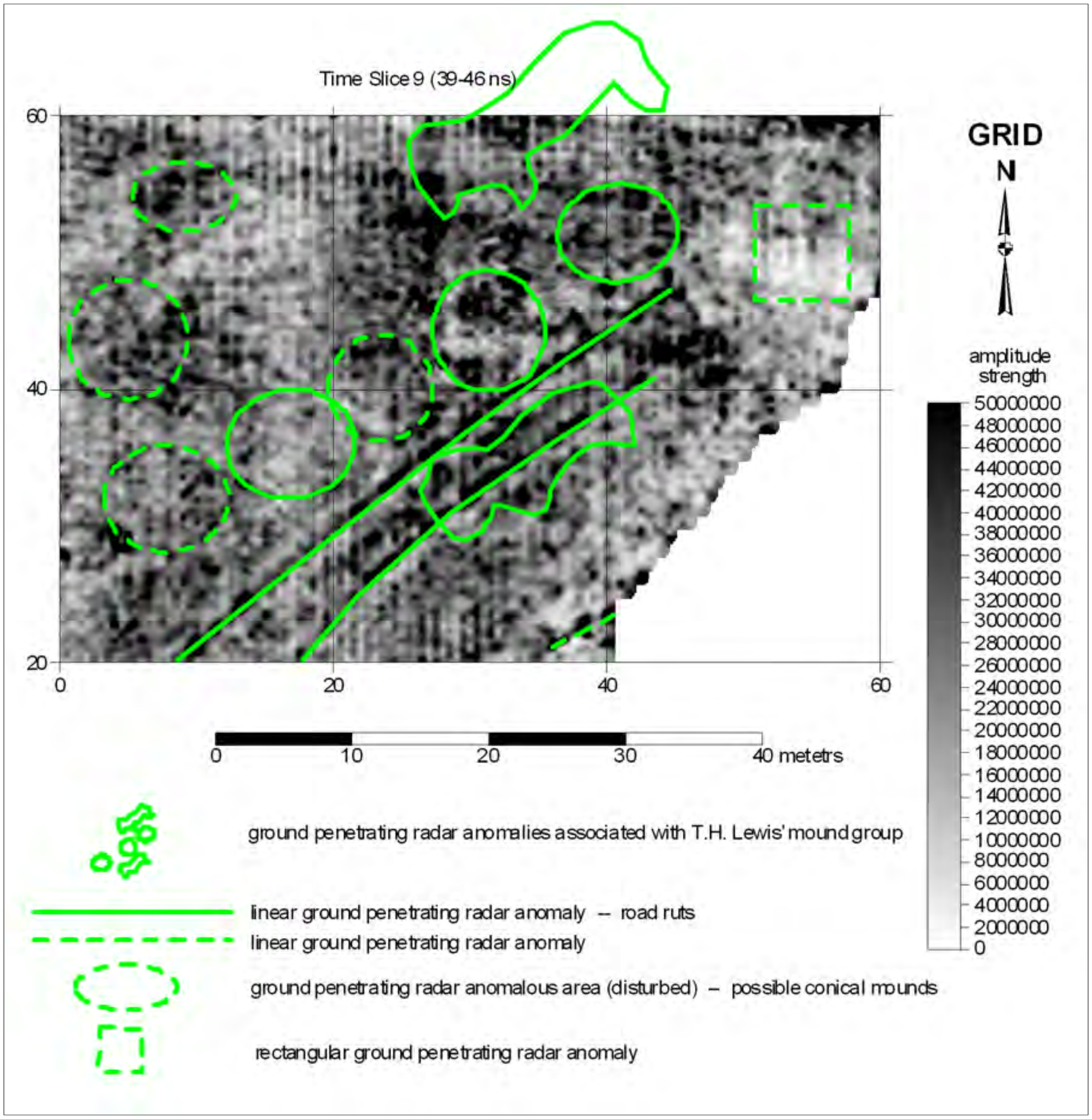

Figure 30. Interpretation of the ground penetrating radar data from time slice 9 (39-46 ns) at the EFMO1 geophysical project area.

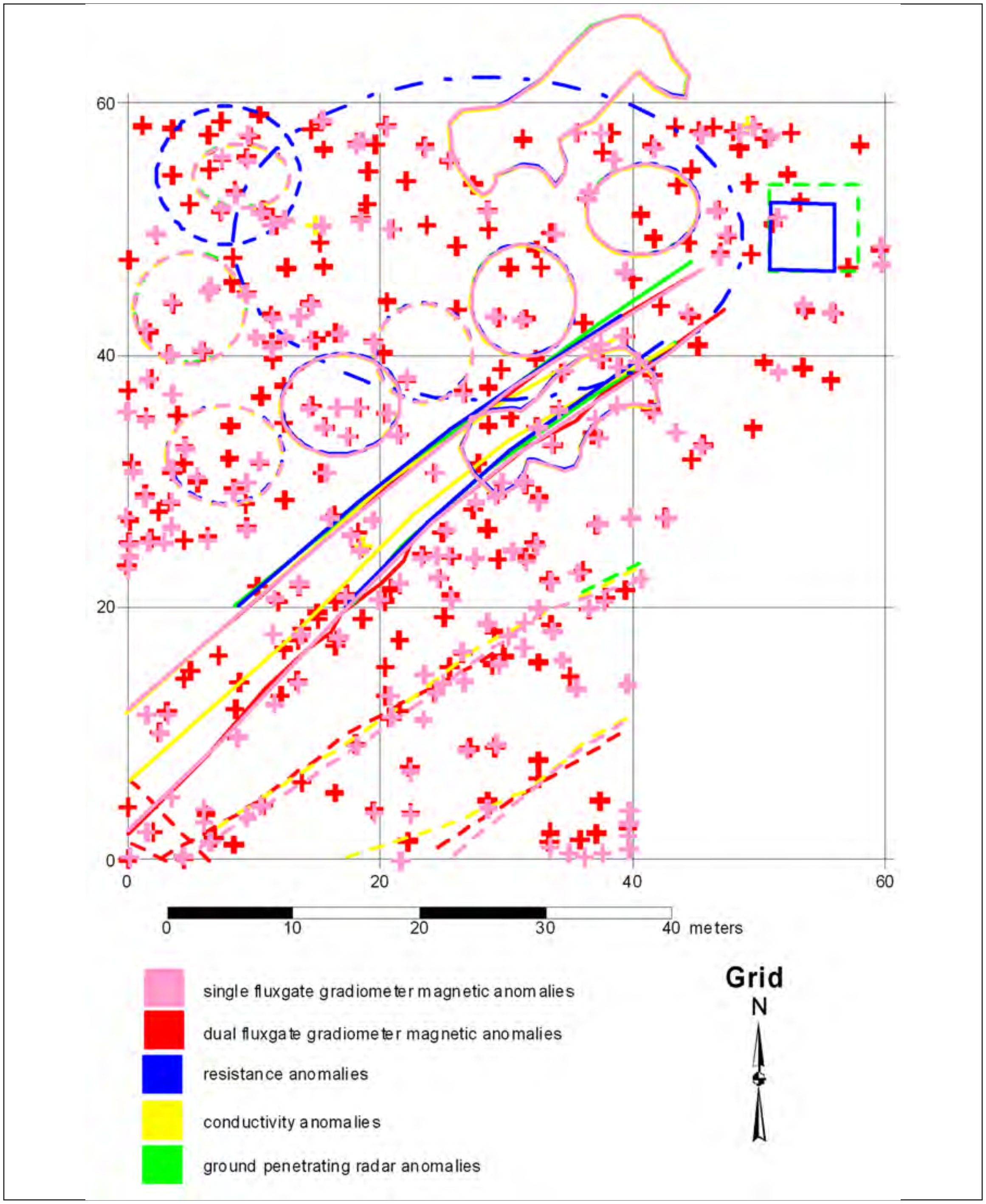

Figure 31. Combined geophysical anomalies from the EFMO2 geophysical project area.

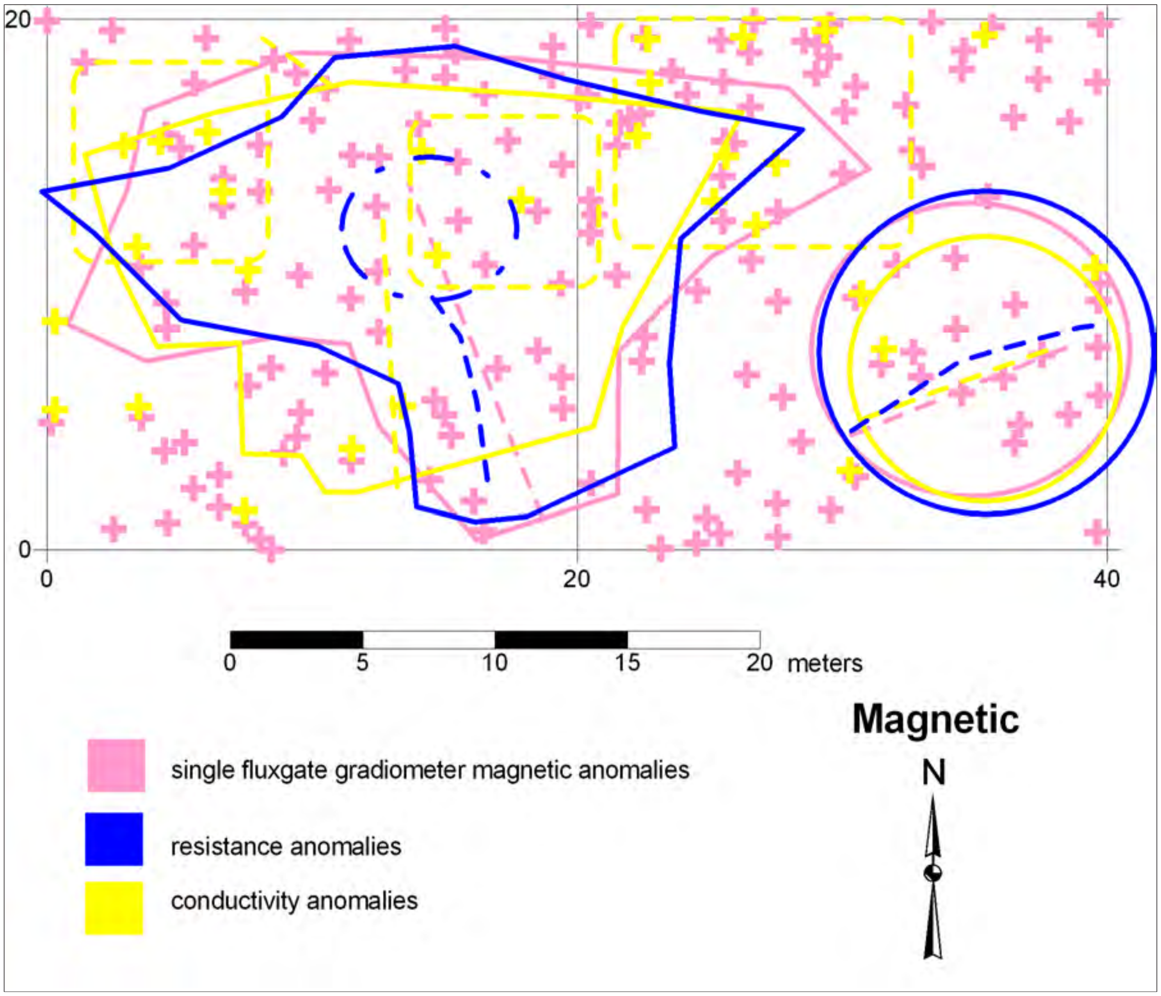

Figure 32. Combined geophysical anomalies from the EFMO2 geophysical project area.